

Discovering E_6 SUSY models in gluino cascade decays at the LHC

Alexander Belyaev,^{1,2,*} Jonathan P. Hall,^{3,†} Stephen F. King,^{1,‡} and Patrik Svantesson^{1,2,§}

¹*School of Physics & Astronomy, University of Southampton, Highfield, Southampton SO17 1BJ, UK*

²*Particle Physics Department, Rutherford Appleton Laboratory, Chilton, Didcot, Oxon OX11 0QX, UK*

³*Physics Department, Indiana University, Bloomington, IN 47405, USA*

We point out that the extra neutralinos and charginos generically appearing in a large class of E_6 inspired models lead to distinctive signatures from gluino cascade decays in comparison to those from the Minimal Supersymmetric Standard Model (MSSM). These signatures involve longer decay chains, more visible transverse energy, higher multiplicities of jets and leptons, and less missing transverse energy than in the MSSM. These features make the gluino harder to discover for certain types of conventional analyses, for example in the 6 jet channel we show that a 1 TeV MSSM gluino may resemble an 800 GeV E_6 gluino. However, the enriched lepton multiplicity provides enhanced 3- and 4-lepton signatures, which are much more suppressed in the case of the MSSM. As an example we analyse various scenarios in the E_6 SSM, demonstrating the utility of a **Ca1cHEP** model that we have now made publicly available on HEPMDB (High Energy Physics Models DataBase). After extensive scans over the parameter space, we focus on representative benchmark points. We perform detailed Monte Carlo analyses, concentrating on the 3-lepton channel at the 7, 8, and 14 TeV Large Hadron Collider (LHC), and demonstrate that E_6 inspired models are clearly distinguishable from the MSSM in gluino cascade decays. We emphasise to the LHC experimental groups that the distinctive features present in gluino cascade decays, such as those discussed here, not only represents a unique footprint of a particular model but also may provide the key to an earlier discovery of supersymmetry.

PACS numbers: 10.14.80.Ly, 10.14.80.Nb, 10.12.60.Jv

* E-mail: a.belyaev@soton.ac.uk

† E-mail: halljp@indiana.edu

‡ E-mail: king@soton.ac.uk

§ E-mail: p.svantesson@soton.ac.uk

CONTENTS

I. Introduction	2
II. Model Setup and Parameter Space	4
A. The E_6 SSM	4
B. Neutralino and chargino mass matrices	5
C. Experimental constraints	7
D. Dark matter considerations	7
E. Parameter space under study	8
F. Benchmarks	11
III. Model Implementation	13
IV. Gluino Production and Decays in the MSSM and E_6 SSM	15
A. Production cross-sections	15
B. Signatures and distributions	16
C. Searches at $\sqrt{s} = 7$ TeV LHC	17
1. 0 leptons	17
2. 1–2 leptons	18
3. 3–4 leptons	20
D. Searches at $\sqrt{s} = 8$ TeV LHC	21
1. 6 jets	21
2. 3 leptons	23
E. 3 lepton searches at $\sqrt{s} = 14$ TeV LHC	24
V. Conclusions	26
Acknowledgments	27
A. Decay Diagrams for Benchmarks	28
B. Details about the CalcHEP Model E6SSM-12.02	32
1. Particle content	32
2. Input parameters	32
3. Functions and dependent parameters	32
4. Feynman rules	35
References	35

I. INTRODUCTION

The general idea of softly broken supersymmetry (SUSY) provides a very attractive framework for physics models beyond the standard model (BSM), in which the hierarchy problem is solved and the unification of gauge couplings can be realised [1]. The simplest such extension, the Minimal Supersymmetric Standard Model (MSSM), has been subjected to particularly close scrutiny at the CERN Large Hadron Collider (LHC). For example, searches at ATLAS [2] and CMS [3, 4], under certain assumptions, constrain the MSSM gluino mass to be greater than about 500–900 GeV. This mass limit range reflects the fact that the precise limit depends crucially on the assumptions one makes about the rest of the SUSY spectrum, in particular the mass spectrum of the squarks, charginos, and neutralinos. As we emphasise in this paper, mass limits and the LHC discovery potential also depend on the particular SUSY model under consideration and the quoted mass limits strictly only apply to the constrained MSSM or simplified models of SUSY[5] with very few particles. In other, well motivated, non-minimal SUSY extensions of the SM, such as those discussed below, the enriched particle content alters the SUSY discovery potential at the LHC and this should be taken into account in the phenomenological and experimental studies.

Despite its many attractive features, the MSSM suffers from the μ problem. The superpotential of the MSSM contains the bilinear term $\mu H_d H_u$, where H_d and H_u are the Higgs doublet superfields. In order to get the correct pattern of electroweak (EW) symmetry breaking the parameter μ is required to be in the TeV region. At the same time, the incorporation of the MSSM into grand unified theories (GUTs) or string theory implies that μ could be of the

order of the GUT or Planck scales, or possibly zero. None of these possibilities is phenomenologically and theoretically acceptable. The Next-to-Minimal Supersymmetric Standard Model (NMSSM) [6] attempts to address this problem by postulating an additional gauge singlet superfield S with the interaction $\lambda SH_d H_u$ in the superpotential together with an S^3 interaction in order to break an accidental global $U(1)$ symmetry to a discrete Z_3 symmetry. At low energies (\sim TeV) the scalar component of S acquires a non-zero vacuum expectation value (VEV) s , giving an effective μ term. However the resulting Z_3 discrete symmetry is broken at the same time, leading to potentially dangerous cosmological domain walls [6].

A solution to the μ problem which does not suffer from the problems of the NMSSM arises within E_6 inspired SUSY models. At high energies the E_6 gauge symmetry arising from GUTs or string theory in extra dimensions can be broken to the rank-5 subgroup $SU(3)_c \times SU(2)_L \times U(1)_Y \times U(1)'$, where in general

$$U(1)' = U(1)_\chi \cos \theta + U(1)_\psi \sin \theta \quad (\text{I.1})$$

and the two anomaly-free $U(1)_\psi$ and $U(1)_\chi$ symmetries originate from the breakings $E_6 \rightarrow SO(10) \times U(1)_\psi$, then $SO(10) \rightarrow SU(5) \times U(1)_\chi$. The extra $U(1)'$ gauge symmetry forbids S^3 interactions since the SM-singlet superfield S is now charged under $U(1)'$. In addition the bilinear μ term is also forbidden if $\theta \neq 0$ or π , while the interaction $\lambda SH_d H_u$ is allowed in the superpotential.

At low energies (\sim TeV) the scalar component of S acquires a non-zero VEV s breaking $U(1)'$ and giving rise to a massive Z' gauge boson together with an effective μ term. Within the class of rank-5, E_6 inspired SUSY models with an extra $U(1)'$ gauge symmetry, there is a unique choice of the extra Abelian gauge group that allows right-handed neutrinos to be uncharged. This is the $U(1)_N$ gauge symmetry given by $\theta = \arctan \sqrt{15}$ [7, 8]. In this particular case, called the Exceptional Supersymmetric Standard Model (E_6 SSM), based on the $SU(3)_c \times SU(2)_L \times U(1)_Y \times U(1)_N$ gauge group, the right-handed neutrinos may be superheavy, allowing a high scale see-saw mechanism in the lepton sector [7, 8].

An elegant feature of the E_6 inspired models with an extra Z' gauge boson at the TeV scale is that the conditions of anomaly cancellation may be satisfied by matter content filling out complete 27 representations of E_6 surviving to the TeV scale. One can therefore have three 27 representations, with each containing a generation of SM matter and fields with the quantum numbers of Higgs doublets and SM-singlets. Thus such models predict, in addition to three SUSY families of quarks and leptons, also three SUSY families of Higgs doublets of type H_u , three SUSY families of Higgs doublets of type H_d , three SUSY SM singlets S_i , and three SUSY families of charge $\mp 1/3$ colour triplet and anti-triplet states D and \bar{D} , which can get large mass terms due to the (third) singlet VEV $\langle S_3 \rangle = s/\sqrt{2}$ which is also responsible for the μ term.

In this paper we study gluino production and decay within the E_6 SSM, expected to be the main discovery channel for this model. In fact the analysis also applies to a larger class of E_6 models in which the matter content of three 27 representations of E_6 survives to the TeV scale. We study the E_6 SSM as a concrete example and at the same time demonstrate the use of the `E6SSM-12.02 CalcHEP` model that we have now made publicly available on HEPMDB. After extensive scans over the parameter space we create a number of representative benchmarks for different E_6 SSM scenarios, considering Z' and Higgs boson physics, the LSP dark matter relic density and direct detection cross-section, and the perturbativity of dimensionless couplings. We then analyse representative MSSM and E_6 SSM benchmarks consistent with the particle recently discovered at the LHC [9, 10] being the SM-like lightest Higgs boson.

The analysis is motivated by the fact that the gluinos are the expected to be the lightest strongly interacting particles in E_6 models [11], so one should expect them to have the largest production rate. In particular, we are interested in gluino cascade decays which not only provide observable signatures, but are also important for distinguishing the E_6 inspired models from the MSSM. As we shall see, there are important differences between the two cases, which can affect the respective search strategies. The differences arise because of the extra Higgsino and singlino states predicted to be part of the E_6 matter content, as above. In particular, in the E_6 inspired models, relative to the MSSM, there are two extra families of Higgsinos, \tilde{H}_u^α and \tilde{H}_d^α , together with two extra singlinos, \tilde{S}^α , where $\alpha = 1, 2$ ¹. There is also a third singlino, \tilde{S}^3 , similar to the NMSSM singlino, which mixes with the bino', both states having a large mass of order the effective μ parameter. The remaining extra Higgsinos and singlinos may be lighter than the gluino. Indeed, it is possible to show that at least two linear combinations of the states \tilde{H}_u^α , \tilde{H}_d^α , \tilde{S}^α must be lighter than or of order $M_Z/2$. If these states mix with the usual neutralinos of the MSSM or NMSSM then the lightest supersymmetric particle (LSP) will inevitably be one of these states, leading to longer decay chains. For example, in regions of MSSM parameter space where the bino is the LSP the gluino typically undergoes a cascade decay to the bino. In the E_6 inspired models the bino will mix with the extra Higgsinos and singlinos and the predominantly bino

¹ Note that the first and second family of Higgs doublet and singlet fields H_u^α , H_d^α , and S^α predicted by the E_6 SSM do not develop VEVs and are called ‘‘inert’’.

state will subsequently decay into some lighter state having a mass of order $M_Z/2$, thereby typically giving a longer gluino cascade decay chain and producing less missing energy due to the lighter mass of the LSP². For simplicity we shall assume that the D and \bar{D} states, as well as the NMSSM type singlino \tilde{S}^3 , are all heavier than the gluino and so are irrelevant for gluino cascade decays. Similarly we shall also assume all squarks and sleptons and Higgs scalars and pseudoscalars (with the exception of the SM-like Higgs boson) to be heavier than the gluino. These assumptions are motivated by the parameter space of the constrained E_6 inspired models [11–13].

The main result of our analysis is that in E_6 inspired models the gluino decays into the LSP with longer chains which involve more jets and leptons and less missing energy than in the MSSM. This happens because the would-be LSP (e.g. an MSSM-like bino dominated neutralino) undergoes further decays to the extra light neutralinos and charginos predicted by the E_6 inspired models. As a result, the characteristics of the signal, such as lepton and jet multiplicity, missing transverse momentum, effective mass, etc., are altered in the E_6 SSM as compared to the MSSM case even after the matching of the gaugino masses in both models. Therefore, the search strategies designed for the MSSM need to be modified for the E_6 SSM case, while one should stress that the gluino mass limits for the MSSM are not applicable to the E_6 SSM gluinos.

The layout of the remainder of this paper is as follows: In section II we summarise the relevant features of the E_6 SSM, its theoretical constraints and its experimental constraints not relating to gluino detection. We also present the results of parameter scans and discuss the viable parameter space, before going on to introduce a set of benchmark points, including those which form the basis of our analysis. The model implementation is discussed in section III (with a more in-depth description of the publicly available code in Appendix B). We then present our analysis of the different signatures and search prospects for different strategies for each model in section IV. The conclusions are in section V.

II. MODEL SETUP AND PARAMETER SPACE

Before going on to consider the prospects for the production and detection of gluinos, which are the main focus of this paper, discussed in section IV, we must first determine the limits on the E_6 SSM from other experimental, and cosmological, considerations. We begin by giving an introduction to the E_6 SSM (subsections II A and II B), explaining the important features. We then discuss experimental constraints relating to Z' and Higgs boson physics and to exotic coloured particles (subsection II C), before going on to discuss dark matter considerations (subsection II D). In light of these discussions we then show the results of some parameter space scans (subsection II E) and produce a set of benchmark points (subsection II F). These benchmarks example various viable scenarios for the E_6 SSM and we explain their features and issues. Although the benchmarks presented look very different from each other from many points of view, it turns out that they look very similar in terms of their gluino decay signatures. In section IV we therefore mostly show results for two particular benchmarks that demonstrate the qualitative differences between the MSSM and E_6 models for gluino searches.

A. The E_6 SSM

As discussed in the Introduction, the E_6 SSM involves a unique choice for the extra Abelian gauge group that allows zero charges for right-handed neutrinos, namely $U(1)_N$. To ensure anomaly cancellation the particle content of the E_6 SSM at the TeV scale is extended to include three complete fundamental 27 representations of E_6 , apart from the three right-handed neutrinos which are singlets and do not contribute to anomalies and so may be much heavier. The 27 representations of E_6 decompose under the $SU(5) \times U(1)_N$ subgroup of E_6 as follows:

$$27_i \rightarrow (10, 1)_i + (5^*, 2)_i + (5^*, -3)_i + (5, -2)_i + (1, 5)_i + (1, 0)_i. \quad (\text{II.1})$$

The first and second quantities in brackets are the $SU(5)$ representation and extra $U(1)_N$ charge (where a GUT normalisation factor of $1/\sqrt{40}$ is omitted [7, 8]) respectively, while i is a family index that runs from 1 to 3. An ordinary SM family, which contains the doublets of left-handed quarks Q_i and leptons L_i , right-handed up- and down-quarks (u_i^c and d_i^c), and right-handed charged leptons is assigned to $(10, 1)_i + (5^*, 2)_i$. Right-handed neutrinos N_i^c should be associated with the last term in Eq. (II.1), $(1, 0)_i$. The next-to-last term, $(1, 5)_i$, represents SM-singlet fields S_i , which carry non-zero $U(1)_N$ charges and therefore survive down to the EW scale. The pair of $SU(2)_L$ -doublets (H_i^d and H_i^u) that are contained in $(5^*, -3)_i$ and $(5, -2)_i$ have the quantum numbers of Higgs doublets.

² The decay to bino is expected to happen before the subsequent decay into a lighter state since these lighter states are expected to have small mixing to the MSSM-like sector, for reasons explained in section II.

They form either Higgs or inert Higgs $SU(2)_L$ multiplets. Other components of these fundamental $SU(5)$ multiplets form colour triplet and anti-triplet of exotic quarks D_i and \bar{D}_i with electric charges $-1/3$ and $+1/3$ respectively. These exotic quark states carry a $B - L$ charge $\mp 2/3$, twice that of ordinary quarks. In addition to the complete 27_i multiplets the low energy matter content of the E_6 SSM can be supplemented by an $SU(2)_L$ doublet L_4 and anti-doublet \bar{L}_4 from extra $27'$ and $\bar{27}'$ representations to preserve gauge coupling unification [14]. These states will typically be much heavier than the gluino and so will play no role in the present analysis, although they may play a role in leptogenesis [15].

As in the MSSM the gauge symmetry in the E_6 SSM does not forbid lepton and baryon number violating operators that result in rapid proton decay, although the situation is somewhat different. The renormalisable superpotential of the E_6 SSM automatically preserves R -parity because of the enlarged gauge symmetry, however, although the $B - L$ violating operators of the R -parity violating MSSM are forbidden by the gauge symmetry, there are new B and L violating interactions involving the new exotic particles. In the E_6 SSM these terms are removed by imposing an exact Z_2 symmetry on the superpotential. There are two options for this symmetry under which the exotic quarks are either interpreted as diquarks or leptoquarks, leading to B and L conservation. Furthermore, the extra particles present in E_6 inspired SUSY models give rise to new Yukawa interactions that in general induce unacceptably large non-diagonal flavour transitions. To suppress these effects in the E_6 SSM an additional approximate Z_2^H symmetry is imposed. Under this symmetry all superfields except one pair of H_d^i and H_u^i (say $H_d \equiv H_d^3$ and $H_u \equiv H_u^3$) and one SM-type singlet field ($S \equiv S^3$) are odd. Ignoring L_4 and \bar{L}_4 , the Z_2^H symmetry reduces the structure of the Yukawa interactions to

$$\begin{aligned}
W_{E_6SSM} \simeq & \lambda \hat{S}(\hat{H}_u \hat{H}_d) + \lambda_{\alpha\beta} \hat{S}(\hat{H}_d^\alpha \hat{H}_u^\beta) + f_{u\alpha\beta} \hat{S}^\alpha(\hat{H}_d^\beta \hat{H}_u) + f_{d\alpha\beta} \hat{S}^\alpha(\hat{H}_d \hat{H}_u^\beta) \\
& + h_{ij}^U(\hat{H}_u \hat{Q}_i) \hat{u}_j^c + h_{ij}^D(\hat{H}_d \hat{Q}_i) \hat{d}_j^c + h_{ij}^E(\hat{H}_d \hat{L}_i) \hat{e}_j^c + h_{ij}^N(\hat{H}_u \hat{L}_i) \hat{N}_j^c \\
& + \frac{1}{2} M_{ij} \hat{N}_i^c \hat{N}_j^c + \kappa_i \hat{S}(\hat{D}_i \hat{\bar{D}}_i),
\end{aligned} \tag{II.2}$$

where hats denote superfields, $\alpha, \beta = 1, 2$ and $i, j = 1, 2, 3$. The inert Higgs doublets and SM-singlets have suppressed couplings to matter, whereas the third generation $SU(2)_L$ doublets \hat{H}_u and \hat{H}_d and SM-type singlet field \hat{S} , that are even under the Z_2^H symmetry, play the role of Higgs fields, radiatively acquiring VEVs. At the physical vacuum their scalar components develop VEVs

$$\langle H_d \rangle = \frac{1}{\sqrt{2}} \begin{pmatrix} v_1 \\ 0 \end{pmatrix}, \quad \langle H_u \rangle = \frac{1}{\sqrt{2}} \begin{pmatrix} 0 \\ v_2 \end{pmatrix}, \quad \langle S \rangle = \frac{s}{\sqrt{2}}, \tag{II.3}$$

generating the masses of the quarks and leptons. Instead of v_1 and v_2 it is more convenient to use $\tan \beta = v_2/v_1$ and $v = \sqrt{v_1^2 + v_2^2} = 246$ GeV. The VEV of the SM-singlet field, s , breaks the extra $U(1)_N$ symmetry, generating exotic fermion masses and also inducing a mass for the Z' boson. Therefore the singlet field S must acquire a large VEV in order to avoid conflict with direct particle searches at present and past accelerators.

We shall assume that the κ_i are sufficiently large that the exotic D_i, \bar{D}_i states are much heavier than the gluino and so will play no role in gluino decays. Similarly the right-handed neutrinos N_i will be neglected since they are assumed to be very heavy.

In this paper we shall be mainly concerned with the first line of Eq. (II.2), namely the couplings of the form $\hat{S}^i \hat{H}_d^j \hat{H}_u^k$, where $i, j, k = 1, 2, 3$ label the three families of Higgs doublet and singlet superfields predicted in the E_6 SSM. In particular we shall be concerned with the resulting chargino and neutralino mass terms coming from such couplings involving one third-family scalar component and two fermion components, i.e. $S \tilde{H}_d^j \tilde{H}_u^k$, $\tilde{S}^i H_d \tilde{H}_u^k$, and $\tilde{S}^i \tilde{H}_d^j H_u$. In the E_6 SSM the presence of the extra Higgsinos and singlinos \tilde{H}_u^α , \tilde{H}_d^α , and \tilde{S}^α means that the chargino and neutralino mass matrices are extended, as discussed in the following subsection.

B. Neutralino and chargino mass matrices

In the MSSM [1] there are four neutralino interaction states, the neutral wino, the bino, and the two neutral Higgsinos. In the USSM [16], a model similar to the NMSSM, but where the $U(1)$ introduced by adding the singlet field S is gauged instead of reduced to a Z_3 , two extra states are added, the singlino and the bino'. In the conventional USSM interaction basis we write the six neutralinos as the column vector

$$\tilde{\chi}_{\text{int}}^0 = (\tilde{B} \quad \tilde{W}^3 \quad \tilde{H}_d^0 \quad \tilde{H}_u^0 \mid \tilde{S} \quad \tilde{B}')^T. \tag{II.4}$$

Neglecting bino-bino' mixing (assumed to be small as justified in Ref. [16]) the USSM neutralino mass matrix in this basis becomes

$$M_{\text{USSM}}^n = \left(\begin{array}{cccc|cc} M_1 & 0 & -m_Z s_W c_\beta & m_Z s_W s_\beta & 0 & 0 \\ 0 & M_2 & m_Z c_W c_\beta & -m_Z c_W s_\beta & 0 & 0 \\ -m_Z s_W c_\beta & m_Z c_W c_\beta & 0 & -\mu & -\mu_s s_\beta & g'_1 v c_\beta Q_d^N \\ m_Z s_W s_\beta & -m_Z c_W s_\beta & -\mu & 0 & -\mu_s c_\beta & g'_1 v s_\beta Q_u^N \\ \hline 0 & 0 & -\mu_s s_\beta & -\mu_s c_\beta & 0 & g'_1 s Q_s^N \\ 0 & 0 & g'_1 v c_\beta Q_d^N & g'_1 v s_\beta Q_u^N & g'_1 s Q_s^N & M'_1 \end{array} \right), \quad (\text{II.5})$$

where M_1 , M_2 , and M'_1 are the soft gaugino masses and $\mu_s = \lambda v / \sqrt{2}$. The variables $s_{\beta(W)}$ and $c_{\beta(W)}$ stand for sin and cos of β (the Weinberg angle) and $Q_{(d,u,S)}^N$ are the $(H_d, H_u, S) U(1)_N$ charges $(-3, -2, 5) / \sqrt{40}$.

In the E_6 SSM the neutralino sector is extended to include the additional six neutral components of \tilde{H}_u^α , \tilde{H}_d^α , and \tilde{S}^α , where $\alpha = 1, 2$. We then take the full list of twelve neutralino interaction states into account in column vector

$$\tilde{\chi}_{\text{int}}^0 = (\tilde{B} \quad \tilde{W}^3 \quad \tilde{H}_d^0 \quad \tilde{H}_u^0 \mid \tilde{S} \quad \tilde{B}' \mid \tilde{H}_{d2}^0 \quad \tilde{H}_{u2}^0 \quad \tilde{S}_2 \mid \tilde{H}_{d1}^0 \quad \tilde{H}_{u1}^0 \quad \tilde{S}_1)^T. \quad (\text{II.6})$$

The first four states are the MSSM interaction states, the \tilde{S} and \tilde{B}' are the extra states added in the USSM, and the final six states are the extra inert doublet Higgsinos and Higgs singlinos that come with the full E_6 SSM. Under the assumption that only the third generation Higgs doublets and singlet acquire VEVs the full Majorana mass matrix is then [17]

$$M_{E_6\text{SSM}}^n = \begin{pmatrix} M_{\text{USSM}}^n & B_2 & B_1 \\ B_2^T & A_{22} & A_{21} \\ B_1^T & A_{21}^T & A_{11} \end{pmatrix}, \quad (\text{II.7})$$

where the sub-matrices involving only the inert interaction states are given by

$$A_{\alpha\beta} = A_{\beta\alpha}^T = -\frac{1}{\sqrt{2}} \begin{pmatrix} 0 & \lambda_{\alpha\beta} s & f_{u\beta\alpha} v \sin \beta \\ \lambda_{\beta\alpha} s & 0 & f_{d\beta\alpha} v \cos \beta \\ f_{u\alpha\beta} v \sin \beta & f_{d\alpha\beta} v \cos \beta & 0 \end{pmatrix} \quad (\text{II.8})$$

and the Z_2^H breaking sub-matrices are given by

$$B_\alpha = -\frac{1}{\sqrt{2}} \begin{pmatrix} 0 & 0 & 0 \\ 0 & 0 & 0 \\ 0 & x_{d\alpha} s & z_\alpha v \sin \beta \\ x_{u\alpha} s & 0 & z_\alpha v \cos \beta \\ x_{u\alpha} v \sin \beta & x_{d\alpha} v \cos \beta & 0 \\ 0 & 0 & 0 \end{pmatrix} \quad (\text{II.9})$$

and involve the small Z_2^H violating Yukawa couplings that were neglected in Eq. (II.2), $x_{u\alpha}$, $x_{d\alpha}$, and z_α . Since these couplings are small,

the inert neutralino sector is only weakly coupled to the USSM sector, and may be considered separately from it to good approximation. However we emphasise that the Z_2^H violating couplings are essential in order for the lightest neutralino from the USSM sector to be able to decay into inert neutralinos and that these couplings are not expected to be zero. Exact Z_2^H would also render exotic D and \bar{D} states stable.

Similarly, we take our basis of chargino interaction states to be

$$\tilde{\chi}_{\text{int}}^\pm = \begin{pmatrix} \tilde{\chi}_{\text{int}}^+ \\ \tilde{\chi}_{\text{int}}^- \end{pmatrix},$$

where

$$\tilde{\chi}_{\text{int}}^+ = \begin{pmatrix} \tilde{W}^+ \\ \tilde{H}_u^+ \\ \tilde{H}_{u2}^+ \\ \tilde{H}_{u1}^+ \end{pmatrix} \quad \text{and} \quad \tilde{\chi}_{\text{int}}^- = \begin{pmatrix} \tilde{W}^- \\ \tilde{H}_d^- \\ \tilde{H}_{d2}^- \\ \tilde{H}_{d1}^- \end{pmatrix}. \quad (\text{II.10})$$

The corresponding mass matrix is then

$$M_{E_6SSM}^c = \begin{pmatrix} & C^T \\ C & \end{pmatrix},$$

where

$$C = \begin{pmatrix} M_2 & \sqrt{2}m_W \sin \beta & 0 & 0 \\ \sqrt{2}m_W \cos \beta & \mu & \frac{1}{\sqrt{2}}x_{d2}s & \frac{1}{\sqrt{2}}x_{d1}s \\ 0 & \frac{1}{\sqrt{2}}x_{u2}s & \frac{1}{\sqrt{2}}\lambda_{22}s & \frac{1}{\sqrt{2}}\lambda_{21}s \\ 0 & \frac{1}{\sqrt{2}}x_{u1}s & \frac{1}{\sqrt{2}}\lambda_{12}s & \frac{1}{\sqrt{2}}\lambda_{11}s \end{pmatrix}. \quad (\text{II.11})$$

It is clear that a generic feature of the E_6SSM is that the LSP is usually (naturally) composed mainly of inert singlino and ends up being typically very light. One can see this by inspecting the new sector blocks of the extended neutralino mass matrix in Eq. (II.7), such as A_{11} , and assuming a hierarchy of the form $\lambda_{\alpha\beta}s \gg f_{u\alpha\beta}v, f_{d\alpha\beta}v$. This is a natural assumption since we already require that $s \gg v$ in order to satisfy the current experimental limit on the Z' mass of around 2 TeV, as discussed below and for example in Ref. [18].

We emphasise again that for both the neutralinos and the charginos we see that if the Z_2^H breaking couplings are exactly zero then the new part of the E_6SSM neutralino mass matrix becomes decoupled from the USSM mass matrix. However, although approximate decoupling is expected, exact decoupling is not, and will therefore not be considered.

C. Experimental constraints

The most recent limit on the $U(1)_N$ Z' mass, set by the CMS [19], searching for dilepton resonances, is $m_{Z'} \gtrsim 1800$ GeV at a confidence level of 95%. Although the limit on the mass of the Z' boson associated with the extra $U(1)_N$ of the E_6SSM can be inferred from this analysis, this analysis neglects any other matter beyond that of the SM. When decays of the Z' boson into inert neutralinos (inert Higgsino and singlino dominated mass eigenstates) are considered the Z' width tends to increase by a factor of about 2 (see for example Ref. [13], although we confirm the result in our analysis). This then means that the branching ratio into leptons is decreased by a factor of about 2. Estimating the effect of halving this expected branching ratio on the analysis in Ref. [19] one can read off a 95% confidence level lower bound of around 1600 GeV. This implies $s \gtrsim 4400$ GeV.

When the singlet VEV is this large, as required, the Higgs boson spectrum typically becomes rather hierarchical with a lightest mass eigenstate that participates in interactions as a SM-like Higgs boson and much heavier Higgs boson states that are approximately decoupled. Indeed the Higgs candidate recently discovered at the LHC can easily be accommodated in the E_6SSM [20]. Although in the MSSM large loop corrections are required in order for this limit to be satisfied, in the E_6SSM this is easier to achieve since there are extra contributions to the SM-like Higgs mass at tree-level due to $U(1)_N$ D-terms.

If the exotic diquarks (or leptoquarks) are light enough

they would produce spectacular signatures at the LHC and these exotic states already have strong limits on their masses. The E_6 diquarks are excluded for masses below 3.5 TeV [21]. Since these particles' masses must be so large they do not play a role in gluino cascade decays and are excluded from our analysis.

D. Dark matter considerations

Stringent constraints on the E_6SSM inert parameter space come from considerations relating to dark matter. In the E_6SSM as described thus far the LSP is typically one of the two necessarily light states from the inert neutralino sector. As such this inert neutralino LSP becomes a dark matter candidate. The E_6SSM has been previously studied as a model attempting to explain the observed amount of thermal relic cold dark matter [17, 22]. Unfortunately this dark matter scenario is now severely challenged by the most recent XENON100 dark matter direct detection limits [23]. The reason is essentially as outlined in the following paragraph and a more detailed analysis can be found in Ref. [22].

In the E_6SSM the LSP is generically singlino dominated, a situation which arises from the extended neutralino mass matrix in Eq. (II.7) under the condition $s \gg v$. One can show that [17, 22] if there is no hierarchy in the Yukawa couplings then the LSP would not annihilate very efficiently at the time of thermal freeze-out and would therefore lead to an unacceptable overabundance of dark matter in the Universe. On the other hand, by allowing the largest $f_{d\alpha\beta}$ and $f_{u\alpha\beta}$ couplings to be significantly larger than the largest $\lambda_{\alpha\beta}$ couplings and $\tan \beta$ to be less than

about 2 the observed amount of dark matter can be predicted. In this case the LSP is heavier and, although still inert singlino dominated, has substantial inert Higgsino admixtures and can annihilate efficiently enough in the early universe via an s-channel Z boson. The largest $\lambda_{\alpha\beta}$ coupling cannot be too small, otherwise the inert charginos would be too light to have so far escaped detection. At the same time the largest $f_{d\alpha\beta}$ and $f_{u\alpha\beta}$ couplings cannot be too large if it is required that perturbation theory remains valid up to the GUT scale. This being the case, the LSP and the NLSP cannot be made much larger than about 60 GeV [22]. In this dark matter scenario there should be some suppression of the coupling of the LSP to the Z boson, by partial cancellation between the up-type and down-type inert Higgsino components, in order to be consistent with the precision measurement of the invisible Z boson width from LEP, if the LSP mass is below half of the Z mass. For given Yukawa couplings increasing $\tan\beta$ has the effect of both suppressing the LSP mass and increasing the coupling to the Z boson, lessening this cancellation. Although this partial cancellation can occur in the coupling of the LSP to the Z boson, the coupling of the LSP to the SM-like Higgs boson is necessarily large if the LSP is to produce the observed amount of dark matter (due to its inert Higgsino admixtures). This in turn means a large spin-independent direct detection cross-section, larger than is now consistent with experiment. However, if the relic abundance is less than the observed value, then the direct detection constraint can be avoided, and that is the strategy that we follow for benchmark points of this kind, as we now discuss in more detail.

It is important to note that for both the MSSM and the standard E_6 SSM we analyse points where less than the observed amount of dark matter is predicted and assume that the majority of dark matter is not made up of MSSM/ E_6 SSM neutralinos. This choice of the parameter space is actually dictated by limits from direct detection experiments: if less than the total amount of the dark matter in the universe is made up of LSPs, then the expected number of events for a direct detection experiment for a given LSP direct detection cross-section will be correspondingly smaller. In the E_6 SSM such points require the previously discussed hierarchy of Yukawa couplings appearing in the inert block of the neutralino mass matrix and in this case if the LSP mass is below half of the Z mass then $\tan\beta$ still cannot be too large in order for the LSP not to contribute too much to the invisible width of the Z boson, as measured at LEP. Large values of $\tan\beta$ mean that the up-type inert Higgsino admixture in the LSP greatly outweighs the down-type inert Higgsino admixture, necessarily leading to a too large coupling to the Z boson.

Alternatively, in a variation of the model known as the EZSSM [24] the situation is quite different and the model may be responsible for all dark matter and consistent with all experiment. Here an extra discrete symmetry Z_2^S is imposed that forbids the terms in the superpotential involving the inert singlet superfields, i.e. the $f_{u\alpha\beta}$ and $f_{d\alpha\beta}$ and Z_2^H violating $x_{u\alpha}$ and $x_{d\alpha}$ Yukawa couplings are forced to be zero. This then means that the inert singlinos are exactly massless and decoupled from the rest of the neutralinos. In this variation of the model the lightest non-inert-singlino LSP is absolutely stable.

If this stable particle is the bino and there are a pair of inert Higgsinos close by in mass then the bino can be responsible for all of dark matter [24]. The massless inert singlinos themselves slightly increase the expansion rate of the universe prior to nucleosynthesis in agreement with observation of the ^4He relic abundance and in this scenario there would currently be a cosmic inert singlino background slightly colder than the cosmic neutrino background [24]. The phenomenology of this scenario as regards the gluino cascade decay is essentially identical to MSSM one and we do not make of point of trying to distinguish this type of scenario from the MSSM in this study.

Finally we shall consider a scenario where the two lightest (predominantly inert singlino) neutralinos are both very light, with one around a GeV, and one much lighter, in principle in the keV range. In this case, interesting phenomenology can emerge in the gluino cascade decays as in the usual case where the lightest neutralino states are around half the Z mass. However, unlike that case, the lightest neutralino is not subject to direct detection limits. Moreover, it is possible to arrange for the correct relic abundance in such a scenario, where the lightest neutralino in the keV mass range is stable and constitutes Warm Dark Matter (WDM) [25]. The idea is that both the light neutralinos are thermally produced in the early Universe due to their couplings to the Z and Z' gauge bosons, but the GeV state decays late (due to its weak couplings) after both of the neutralinos have gone out of thermal equilibrium, and reheats the Early Universe, effectively diluting the number density of the stable keV neutralinos, such that they are responsible for the observed relic abundance. It is very interesting to compare the gluino cascade decays in this case to that where the lightest neutralinos are around half the Z mass, in order to provide an experimental ‘‘confirmation’’ of keV dark matter at the LHC.

E. Parameter space under study

In this study we consider a pattern of low energy soft gaugino masses that is consistent with E_6 grand unification [7]. This typically implies that at the EWSB scale $M_2 \approx 2M_1$ and if $M_1 = 150$ GeV the physical gluino mass is around 800 GeV. In order to have a direct comparison, M_1 is made equal in both the MSSM and E_6 SSM, 150 GeV in the following analysis. We also fix the physical gluino mass to be equal, 800 GeV in the following analysis. For large

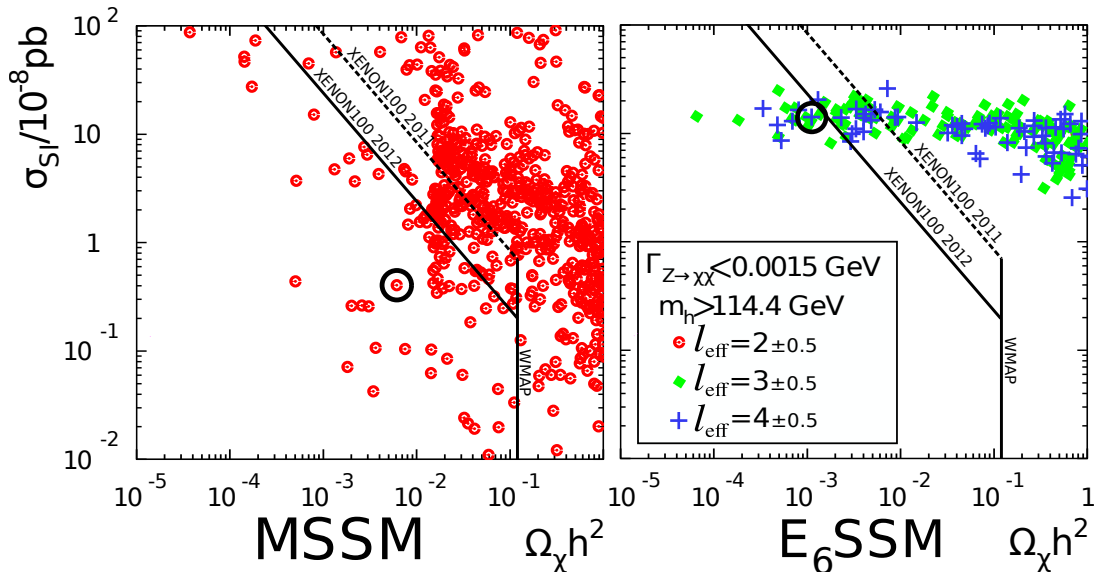


FIG. 1. The scanned regions of the parameter spaces projected onto the plane spanned by the spin-independent cross-section, σ_{SI} , and the relic density of the LSP, $\Omega_{\tilde{\chi}_1^0} h^2$. The area right of the vertical solid line is excluded by WMAP [26] and the area above the diagonal line is excluded by XENON100, where the LSP direct detection cross-section exclusion gets weighted by its relic density. The 90% confidence level limit on the spin-independent LSP-nucleon cross section for a weakly interacting LSP with mass around 50 GeV and which makes up all of the observed amount of DM has been pushed down from $0.7 \times 10^{-44} \text{cm}^2 = 0.7 \times 10^{-8} \text{pb}$ in 2011 [23] to $0.2 \times 10^{-44} \text{cm}^2 = 0.2 \times 10^{-8} \text{pb}$ in 2012 [27]. The LEP constraints on chargino masses ($m_{\tilde{\chi}_{1\pm}} > 103 \text{ GeV}$) and invisible Z width ($\Gamma(Z \rightarrow \tilde{\chi}^0 \tilde{\chi}^0) < 1.5 \text{ MeV}$) have been applied. The constraint on the Higgs mass is also taken from LEP since it holds for invisible Higgs decays, a common feature among the $E_6\text{SSM}$ points. The colours/shapes represent the effective gluino decay chain length $l_{\text{eff}} = \sum_l l \cdot P(l)$ for each point, where $P(l)$ is the probability for a chain length of l , as defined in Fig. 2. The benchmarks entitled MSSM and $E_6\text{SSM-I}$, which are consistent with the particle recently discovered at the LHC being the SM-like lightest Higgs boson, are encircled.

μ in the MSSM, and given that the effective μ in the $E_6\text{SSM}$ is large due to the limit on s coming from the limit on the Z' mass, there will be a neutralino that is almost the bino with a mass very close to M_1 . For lower values of μ in the MSSM bino-Higgsino mixing occurs.

We also consider large squark masses, with all squarks heavier than the gluino. This is motivated by the GUT constrained $E_6\text{SSM}$, where such large squark masses are a feature, although it should be noted that although the EZSSM scenario is consistent with such GUT constraints it has not been shown that a GUT constrained standard $E_6\text{SSM}$ scenario consistent with dark matter observations exists. Nonetheless we assume heavy squarks for all scenarios.

In Fig. 1 we present the results of scans over the MSSM and the $E_6\text{SSM}$ parameter space in the $(\Omega_{\tilde{\chi}_1^0} h^2, \sigma_{SI})$ plane. The parameter space scanned over is shown in Tabs. I and II and points are linearly distributed over these ranges. The ranges chosen are motivated from the discussions in the previous two subsections. For both the MSSM and $E_6\text{SSM}$ the points are shown as long as they are consistent with the LEP limit on the SM-like Higgs boson mass, applicable even if the Higgs has large invisible branching fractions, but we also highlight benchmark points that are consistent with the particle recently discovered at the LHC being the SM-like lightest Higgs boson. For the $E_6\text{SSM}$, where the LSP mass may be less than half of the Z mass, points are only shown if they are consistent with LEP limits on the invisible Z width, contributing less than 1-sigma. For both scans squark soft masses are set to 2 TeV, although the effects of squark mixing on the mass eigenstates are included. The physical gluino mass is set to 800 GeV and the $U(1)_Y$ gaugino mass is set to 150 GeV in both cases. We do not consider scenarios in which any squarks are less massive than the gluino.

We define the length of a gluino decay chain to be the number of decays after the virtual squark as in Fig. 2. We then also define an effective chain length for each point in parameter space

$$l_{\text{eff}} = \sum_l l \cdot P(l), \quad (\text{II.12})$$

where $P(l)$ is the probability of having a decay chain of length l for that point. Intervals of effective chain length are colour/shape coded in Fig. 1. These scans indicate that in the $E_6\text{SSM}$ these decay chains are typically longer due to the bino decaying into the lower mass inert states. The distribution of effective chain lengths for these scans are also

parameter	min	max
$\tan\beta$	2	60
$A_t = A_b = A_\tau = A_\mu$	-3	3
M_A	0.1	2
μ	-2	2

TABLE I. The MSSM scanning region. A common squark and slepton mass scale was fixed to $M_S = 2$ TeV. The gaugino masses were fixed to $M_1 = 150$ GeV, $M_2 = 285$ GeV, and $M_3 = 619$ GeV, providing a gluino mass close to 800 GeV.

parameter	min	max
$\tan\beta$	1.4	2
$ \lambda $	0.3	0.7
λ_{22}	0.0001	0.01
λ_{21}	0.01	0.1
λ_{12}	0.01	0.1
λ_{11}	0.0001	0.01
f_{d21}	0.0001	0.01
f_{d21}	0.1	1
f_{d12}	0.1	1
f_{d11}	0.0001	0.01
f_{u22}	0.0001	0.01
f_{u21}	0.1	1
f_{u12}	0.1	1
f_{u11}	0.0001	0.01
x_{d2}	10^{-4}	10^{-2}
x_{d1}	10^{-4}	10^{-2}
x_{u2}	10^{-4}	10^{-2}
x_{u1}	10^{-4}	10^{-2}
z_1	10^{-3}	10^{-1}
z_2	10^{-3}	10^{-1}
$A_t = A_b = A_\tau$	-3	3
M_A	1	5
s	3.7	8

TABLE II. The E_6 SSM scanning region. A common squark and slepton mass scale was fixed to $M_S = 2$ TeV. The gaugino masses were fixed to $M_1 = 150$ GeV, $M'_1 = 150$ GeV, $M_2 = 300$ GeV, and $M_{\tilde{g}} = 800$ GeV.

plotted in Fig. 3(a).

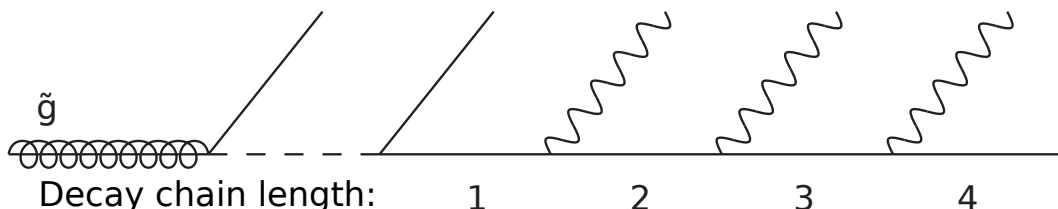
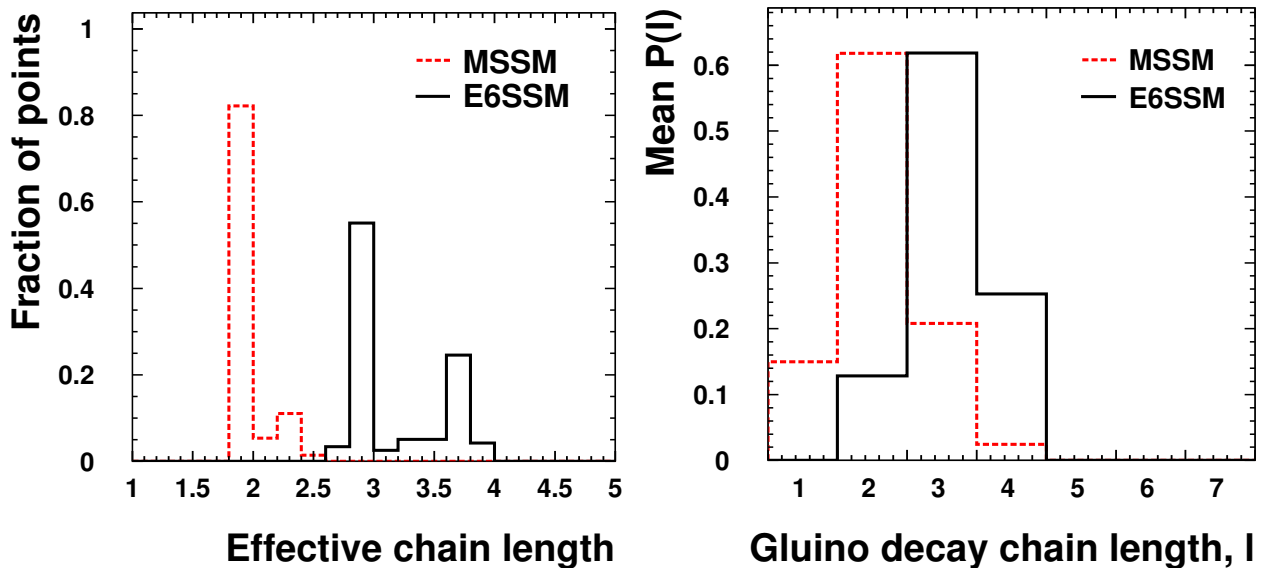


FIG. 2. In the first step in a gluino decay chain the gluino decays into a quark and a squark (in our scenario it will be a virtual squark) which in turn decays into a second quark and a neutralino or chargino. This is the shortest possible gluino decay chain, which we define as having length $l = 1$. The neutralino or chargino can then decay into lighter neutralinos or charginos by radiating W , Z , or Higgs bosons, which typically decay into pairs of fermions. For each such decay the decay chain length is taken to increase by one. The radiated bosons could be on-shell or off-shell depending on the mass spectrum of the model. Light squarks or leptons could appear further along in the decay chain, leading to radiation of SM fermions without intermediate W , Z , or Higgs bosons, but in our study squarks and sleptons are heavy so this is not relevant.

In the MSSM, for the parameters chosen, the typical decay length is 2, with the lightest chargino being initially produced from the virtual squark decay before subsequently itself decaying to the bino LSP. When the magnitude of μ is small the mixing between the gauginos (bino and wino) and the Higgsinos increases and the entire neutralino and chargino spectrum is pushed down. Specifically the heavier neutralinos and chargino are brought down below the gluino mass causing extra steps in the gluino decay chain.

In the E_6 SSM the effective decay length is typically either 3 or 4. Initially an either charged or neutral wino is produced and this subsequently decays to the bino. The bino then decays into either of the two light inert neutralinos that are the LSP and NLSP. Which of these the bino preferentially decays into depends on the values of the Z_2^H violating couplings in blocks B_α in the neutralino mass matrix in Eq. (II.7). Therefore in the E_6 SSM we typically expect the gluino cascade decays to be either one or two steps longer than in the MSSM.



(a) The distribution of the effective chain length, $l_{\text{eff}} = \sum_l l \cdot P(l)$, where $P(l)$ is the probability of having a decay chain of length l for a point in parameter space.

(b) The probability for a certain gluino decay chain length, averaged over all points in the parameter scan, satisfying dark matter and collider constraints.

FIG. 3. Statistical properties of the gluino decay chain length in the scanned parameter space. Figure 3(a) shows how the effective gluino decay chain length evaluated at each point is distributed over the scanned parameter space. Most points have an effective decay chain length close to an integer indicating that there usually is a largely dominant decay chain length. The two peaks just below 3 and 4 clearly show how the E_6 SSM generally introduces one or two extra steps in the chain. Figure 3(b) shows the average probabilities of different gluino decay chain lengths for both models' parameter spaces. Again, the E_6 SSM is shown to shift the probabilities to longer decay chain lengths.

F. Benchmarks

Below follow descriptions of the main features of the chosen benchmarks. The details of their spectrum and parameter values are given in Tab. III. The diagrams for the main decay channels of the gluinos are shown in Fig. 4 for two main benchmarks, MSSM and E_6 SSM-I discussed below. The branching ratios for production of particles are denoted in brackets. The decay chains for both benchmarks are essentially the same up to the first two steps, with just a slight difference in branching ratios. The essential difference is that, in the case of the E_6 SSM, the lightest MSSM-like neutralino is no longer stable and decays in two steps to the lightest E_6 SSM neutralino. About 20% of the gluino decays go directly into the lightest MSSM-like neutralino implying a chain length $l = 1$ for the MSSM and $l = 3$ for the E_6 SSM. On the other hand, about 80% of the gluino decays are into a heavier neutralino or chargino, which subsequently decays into the lightest MSSM-like neutralino state giving the MSSM a chain length $l = 2$ and the E_6 SSM $l = 4$. More complete diagrams showing how the gluinos decay for the different benchmarks (below) are shown in Fig. 15 in Appendix A.

The following benchmarks provide the main focus of our study:

- MSSM:

In this benchmark we have an LSP with a mass of 150 GeV. The low dark matter relic density is achieved via LSP resonance annihilation through the CP-odd and heavy Higgs bosons, A and H . The lightest Higgs boson, h , has a mass of 124.4 GeV and can be produced in gluino decay chains. This happens when the gluino decays via the next to lightest neutralino $\tilde{\chi}_2^0$. The gluino decay chain length is dominantly $l = 2$ for this benchmark as for all the MSSM points scanned over.

- E_6 SSM-I:

In this benchmark the LSP and NLSP annihilate efficiently through the Higgs boson resonance leaving a relic density less than the observed relic density of dark matter. The lightest Higgs mass is around 125 GeV and the two lightest inert neutralino state masses are slightly above half of the Higgs mass. In this case the Higgs is SM-like in both its composition and its decays, since only decays into SM final states are kinematically allowed. If the LSP mass was be slightly below half of the Higgs mass then the Higgs boson would decay invisibly. In order for the two lightest inert neutralino states to be heavy enough some of the $f_{u\alpha\beta}$ and $f_{d\alpha\beta}$ are required to be

MSSM:

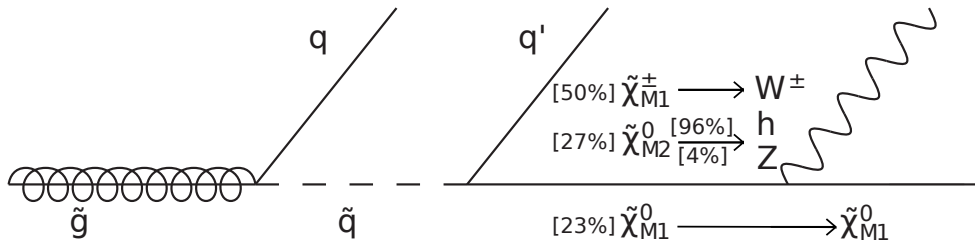
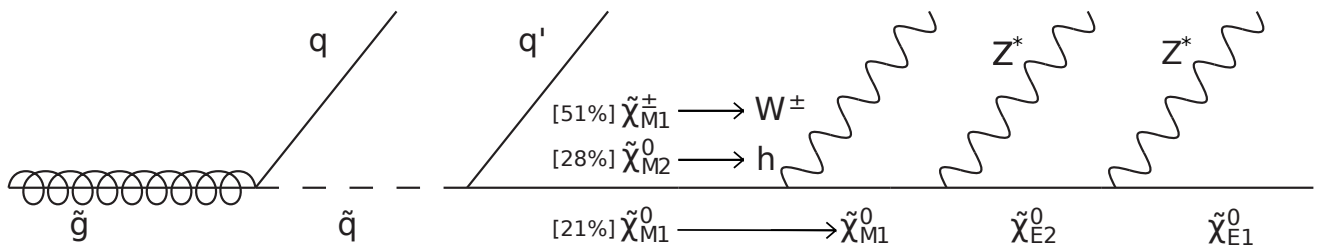
E₆SSM-I:

FIG. 4. Feynman diagrams for the leading gluino decay chains for our two main benchmarks, MSSM and E₆SSM-I. The branching ratios for production of particles are denoted in brackets. The decay chains for both benchmarks are essentially the same up to the first two steps, with just a slight difference in branching ratios. The essential difference is that, in the case of the E₆SSM, the lightest MSSM-like neutralino is no longer stable and decays in two steps to the lightest E₆SSM neutralino. About 20% of the gluino decays go directly into the lightest MSSM-like neutralino implying a chain length $l = 1$ for the MSSM and $l = 3$ for the E₆SSM. On the other hand, about 80% of the gluino decays into a heavier neutralino or chargino, which subsequently decays into the lightest MSSM-like neutralino state, giving the MSSM a chain length $l = 2$ and the E₆SSM $l = 4$.

large enough such that Yukawa coupling running becomes non-perturbative on the way up to the GUT scale. We estimate that here the Yukawa couplings remain perturbative up to an energy scale of order 10^{12} GeV. Compared to the MSSM benchmark there are typically two extra steps in the decay chain as the bino-like neutralino decays into first the NLSP which subsequently decays into the LSP. The two extra steps in the chain make the most common total gluino decay chain length $l = 4$. The decay of the bino into the NLSP is preferred over the decay directly into the LSP because of the structure of the Z_2^H breaking trilinear Higgs Yukawa couplings given in Tab. IV.

- E₆SSM-II:

This benchmark represents a typical scenario, with decay chain features similar to in the E₆SSM-I benchmark, where the most common decay length is 4. Yukawa coupling running remains perturbative up to the GUT scale, as it does in all of the following benchmarks. Just as in previous benchmark the gluino decay chain length here is typically two steps longer than in the MSSM because of the two extra light neutralino states, but here their masses are smaller. The LSP mass is below half of the Z boson mass, but decays of the Z boson into LSP-LSP contribute to the effective number of neutrinos as measured at LEP less than 1-sigma. Because the LSP and NLSP have masses not very far away from half of the Z mass they are able to annihilate relatively efficiently via an s-channel Z boson in the early Universe and the LSP contributes much less than the observed relic density of dark matter. This benchmark has a rather heavy lightest Higgs with a mass around 134 GeV. This Higgs decays dominantly invisibly into a pair LSPs and is ruled out if the boson candidate discovered at the LHC is interpreted as a SM-like Higgs boson.

- E₆SSM-III:

In contrast to previous benchmarks this benchmark represents the other typical E₆SSM scenario where the bino-like neutralino decays straight to the LSP (not via the NLSP). In this case there is only one extra step compared to the MSSM and the most common decay length is 3. Points with this shorter decay length are slightly more common when one scans over the Z_2^H breaking Yukawa couplings. In the same way as in E₆SSM-II the LSP annihilates efficiently via an s-channel Z boson, even though it is farther away from resonance, and contributes much less than the observed relic density of dark matter. In this benchmark the lightest Higgs has a mass around 116 GeV, much lighter than in E₆SSM-II. As above, this is ruled out if the boson candidate discovered at the LHC is interpreted as a SM-like Higgs boson. This benchmark represent the slightly more

common scenario in the parameter space where the typical decay chain has one extra step after the 150 GeV bino-like neutralino.

- E_6 SSM-IV (EZSSM-I):

This benchmark represents an EZSSM dark matter scenario as described in Ref. [24]. Here the bino-like neutralino is stable and makes up all of the observed dark matter relic density. A low enough relic density is achieved via the bino-like neutralino upscattering into the inert Higgsino pseudo-Dirac pair $\tilde{\chi}_{E_3}^0$ and $\tilde{\chi}_{E_4}^0$. Since the bino is stable the gluino decays of this benchmark are essentially identical to those of the MSSM benchmark and also have the same dominant decay chain length $l = 2$. The bino-like neutralino's direct detection cross-section is small.

This benchmark looks very similar to the MSSM benchmark and cannot be distinguished from it purely by analysis of gluino cascade decays. However, if a heavy or CP-odd Higgs around 300 GeV was to be excluded then the MSSM, but not the EZSSM, benchmark would be excluded. This relies on the fact that the EZSSM can have a stable bino at 150 GeV without requiring resonance annihilation through heavy Higgs boson states, which in contrast is required in the MSSM. The Higgs boson has a mass around 125 GeV and is SM-like in its composition and decays.

- E_6 SSM-V (EZSSM-II):

This is another benchmark of the EZSSM, but here the dark matter relic density is not explained. Here the inert Higgsino pseudo-Dirac pair have masses around 120 GeV, well below the bino-like neutralino. These states co-annihilate efficiently in the early universe and contribute a dark matter relic density less than the total observed dark matter relic density. The effective decay chain length is about 4. The complete decay modes for the gluino are shown in Fig. 15(f) in Appendix A. This benchmark provides an example of heavier lightest inert neutralino masses (excluding the decoupled inert singlinos) without requiring non-perturbatively large Yukawa couplings as in the non-EZSSM benchmark E_6 SSM-I. Because the lightest inert-Higgsino-like neutralinos have masses much larger than half of the lightest Higgs mass, which is 126 GeV, the Higgs will decay very SM-like.

- E_6 SSM-VI (approximate Z_2^S):

In this benchmark the inert singlino decoupling is not exact and the inert singlino-like LSP mass is not zero, but has been pushed down to the 100 keV scale. This point represents the scenario where the lightest neutralino in the keV mass range is stable and constitutes Warm Dark Matter (WDM) [25], as described earlier, although we do not calculate the relic density here.

The approximate decoupling leads to a quite long-lived bino (with a width of order 10^{-11} GeV) and the step in the decay after the bino appears as a displaced vertex at the order of 0.1 mm from the previous step. The decay chain length is typically 4. The complete decay modes for the gluino is shown in Fig. 15(g) in Appendix A. As remarked, the observed relic density could be achieved by pushing the LSP mass down to the keV scale. In this case the last steps of the gluino decay would be likely to occur outside the detector and one would be left with something that looks like the MSSM. The lightest Higgs has a mass of 126 GeV and decays to the LSP are very suppressed due to its small mass. The Higgs could decay to the GeV scale NLSP, which in turn would decay to the LSP outside the detector since its width is of the order 10^{-20} GeV, leading to invisible Higgs decays. The branching ratio for $h \rightarrow \tilde{\chi}_2^0 \tilde{\chi}_2^0$ is however around 6% and is not excluded by current Higgs data.

In the following analysis, in section IV, we use MSSM and E_6 SSM-I as our main benchmarks. With the exception of E_6 SSM-IV (EZSSM-I) the results obtained for each of the E_6 SSM benchmarks are very similar. (E_6 SSM-IV on the other hand looks very similar to the MSSM, since the bino is stable.) We therefore mainly give just the results for MSSM and E_6 SSM-I, demonstrating the qualitative difference between the MSSM and E_6 models. We also include some results for the E_6 SSM-VI to demonstrate the effects of having an even less compact spectrum and also to show how little our conclusions depend on the exact spectrum of the E_6 model.

III. MODEL IMPLEMENTATION

To scan parameter spaces of models and generate Monte Carlo events the models have to be transferred from paper to computer. There are various ways of doing this. Many implementations of the MSSM have already been created, but for the E_6 SSM there are no available sources. We have chosen to use the software package **LanHEP** [28] to calculate the Feynman rules for the E_6 SSM. **LanHEP** finds the interactions and mass mixings between the particle states in the model and writes an output which can be read by a Feynman diagram calculator or Monte Carlo event generator. **LanHEP** can output in several formats. We have been using the format used by **CalcHEP** since that is the software we are using for calculating Feynman diagrams and generating events.

	MSSM	E ₆ SSM-I	E ₆ SSM-II	E ₆ SSM-III	E ₆ SSM-IV	E ₆ SSM-V	E ₆ SSM-VI	
$\tan\beta$	10	1.5	1.42	1.77	3	1.42	1.42	
λ	-	0.497	0.598	-0.462	-0.4	0.598	0.598	
s	-	5180	5268	5418	5500	5268	5268	
μ	1578	(1820)	(2228)	(1770)	(-1556)	(2228)	(2228)	
$A_t = A_b = A_\tau$	-2900	-3110	-3100	476.2	4638	-2684	-2684	
M_A	302.5	3666	4365	2074	4341	4010	4000	[GeV]
M_1	150	150	150	150	150	150	150	
M_2	285	300	300	300	300	300	300	
$M_{1'}$	-	151	151	151	151	151	151	
$m_{\tilde{g}}$	800.2	800.0	800.0	800.0	800.0	800.0	800.0	
$m_{\tilde{\chi}_{M1}^0}$	148.7	148.9	149.1	151.2	150.6	149.1	149.1	
$m_{\tilde{\chi}_{M2}^0}$	302.2	296.1	296.8	303.7	301.7	296.8	296.8	
$m_{\tilde{\chi}_{M3}^0}$	1582	1763	2233	1766	1557	2233	2233	
$m_{\tilde{\chi}_{M4}^0}$	1584	1823	2246	1771	1558	2246	2246	
$m_{\tilde{\chi}_{M1}^\pm}$	302.2	299.0	299.2	300.9	300.4	299.2	299.2	
$m_{\tilde{\chi}_{M2}^\pm}$	1584	1822	2229	1771	1557	2229	2229	
$m_{\tilde{\chi}_{U1}^0}$	-	1878	1835	1909	1937	1835	1835	[GeV]
$m_{\tilde{\chi}_{U2}^0}$	-	1973	2003	2062	2087	2003	2003	
$m_{\tilde{\chi}_{E1}^0}$	-	62.7	43.5	45.2	0	0	0.00011	
$m_{\tilde{\chi}_{E2}^0}$	-	62.8	48.6	53.2	0	0	1.53	
$m_{\tilde{\chi}_{E3}^0}$	-	119.8	131.3	141.6	164.1	119.9	120.1	
$m_{\tilde{\chi}_{E4}^0}$	-	121.0	163.6	187.4	164.1	119.9	122.8	
$m_{\tilde{\chi}_{E5}^0}$	-	183.0	197.0	227.8	388.9	185.8	185.8	
$m_{\tilde{\chi}_{E6}^0}$	-	184.4	224.3	265.6	388.9	185.8	187.0	
$m_{\tilde{\chi}_{E1}^\pm}$	-	109.8	119.9	122.7	164.1	119.9	119.9	
$m_{\tilde{\chi}_{E2}^\pm}$	-	117.7	185.8	225.1	388.9	185.8	185.8	
m_h	124.4	125.4	133.8	116.3	124.7	126.1	125.8	
$P(l=1)$	0.188	$< 10^{-9}$	$< 10^{-5}$	$< 10^{-5}$	0.1727	$< 10^{-8}$	$< 10^{-12}$	
$P(l=2)$	0.812	$< 10^{-4}$	0.01524	0.1723	0.8273	0.01	$< 10^{-5}$	
$P(l=3)$	0	0.1746	0.2336	0.7986	$< 10^{-6}$	0.2	0.1721	
$P(l=4)$	0	0.8196	0.7512	0.02915	$< 10^{-15}$	0.8	0.8280	
$P(l=5)$	0	0.0058	$< 10^{-7}$	0	0	$< 10^{-15}$	0	
Ωh^2	0.00628	0.00114	0.0006842	0.0006937	0.101	0.00154		
σ_{SI}	0.401×10^{-9}	15.34×10^{-8}	9.35×10^{-8}	16.35×10^{-8}	3.75×10^{-11}	3.98×10^{-13}		[pb]

TABLE III. Benchmarks motivated by the parameter scans presented in Fig. 1 and Tabs. I and II. From top to bottom the classes of parameters are dimensionless input parameters; dimensionful input parameters; neutralino, chargino, and lightest Higgs masses (in absolute values); probabilities for certain gluino decay chain lengths; and finally dark matter properties. The $\tilde{\chi}_{Mi}^{0(\pm)}$ are MSSM-like states, the $\tilde{\chi}_{Ui}^0$ are USSM-like states, being mainly mixtures of \tilde{S} and \tilde{B}' . The $\tilde{\chi}_{Ei}^{0(\pm)}$ are states introduced by the inert sector of E₆SSM. The scale for squark and slepton masses is $M_S = 2$ TeV in all benchmarks.

In the **LanHEP** implementation of the model the particle content and Lagrangian is specified. We have used a slightly stripped down version of the E₆SSM, suitable for our purposes. What is not included from the three families of 27 representations of the E₆ group are the exotic coloured states ³, their superpartners, and the inert Higgs doublets and SM-singlets, from the two first families. However, one should note that we are including the superpartners of these inert Higgs and singlet states which, as described in section II B, extends the neutralino and chargino sectors. The diagonalisation of large mass matrices appearing in the model, e.g. the 12×12 neutralino mass matrix, is performed with routines available from the **SLHAp1us** [29] package which is well integrated with **LanHEP** and **CalcHEP**.

The Z_2^H violating Yukawa couplings, x_u , x_d , and z , connecting the inert neutralino sector with the USSM sector, have been included in the **LanHEP** model. Turning on these couplings causes the neutralino mass matrix to leave its block-diagonal form and acquire non-zero off-block-diagonal elements. The model is parameterised such that the dimensionless input parameters are the Yukawa couplings λ_{ijk} from the $\hat{S}\hat{H}_u\hat{H}_d$ -terms in the superpotential, the ratio of the Higgs doublet VEVs, $\tan\beta$, and the gauge couplings. Dimensionful input parameters of the model are the third generation soft trilinear scalar A-couplings, the soft masses of the squarks and sleptons, and the soft gaugino masses

³ These can be diquarks or leptoquarks depending on the model definition.

	E ₆ SSM-I	E ₆ SSM-II	E ₆ SSM-III	E ₆ SSM-IV	E ₆ SSM-V	E ₆ SSM-VI
λ	3.93×10^{-1}	5.98×10^{-1}	-4.77×10^{-1}	-4.0×10^{-1}	5.98×10^{-1}	5.98×10^{-1}
λ_{22}	-3.57×10^{-4}	-4.48×10^{-3}	5.14×10^{-3}	1.0×10^{-1}	-4.48×10^{-3}	-4.48×10^{-3}
λ_{21}	3.0×10^{-2}	-4.34×10^{-2}	-8.77×10^{-2}	0	-4.34×10^{-2}	-4.34×10^{-2}
λ_{12}	3.21×10^{-2}	-3.83×10^{-2}	6.40×10^{-2}	0	-3.83×10^{-2}	-3.83×10^{-2}
λ_{11}	7.14×10^{-4}	-1.25×10^{-2}	-3.36×10^{-2}	4.22×10^{-2}	-1.25×10^{-2}	-1.25×10^{-2}
f_{d22}	1×10^{-3}	-9.02×10^{-3}	7.06×10^{-3}	0	0	2.0×10^{-1}
f_{d21}	6.844×10^{-1}	-3.48×10^{-1}	6.10×10^{-1}	0	0	-3.48×10^{-3}
f_{d12}	6.5×10^{-1}	6.92×10^{-1}	-7.64×10^{-1}	0	0	6.92×10^{-3}
f_{d11}	1×10^{-3}	6.17×10^{-3}	9.26×10^{-3}	0	0	6.17×10^{-5}
f_{u22}	1×10^{-3}	-6.77×10^{-3}	3.93×10^{-3}	0	0	1.0×10^{-1}
f_{u21}	6.7×10^{-1}	-7.86×10^{-1}	-8.56×10^{-1}	0	0	-7.86×10^{-3}
f_{u12}	6.4×10^{-1}	2.52×10^{-1}	-2.71×10^{-1}	0	0	2.52×10^{-3}
f_{u11}	1×10^{-3}	8.59×10^{-3}	-2.24×10^{-3}	0	0	8.59×10^{-5}
x_{d2}	7.14×10^{-4}	4.04×10^{-3}	2.35×10^{-4}	4.04×10^{-5}	4.04×10^{-5}	4.04×10^{-5}
x_{d1}	7.14×10^{-4}	5.11×10^{-4}	2.96×10^{-4}	5.11×10^{-6}	5.11×10^{-6}	5.11×10^{-6}
x_{u2}	7.14×10^{-4}	-2.01×10^{-3}	9.04×10^{-4}	-2.01×10^{-5}	-2.01×10^{-5}	-2.01×10^{-5}
x_{u1}	7.14×10^{-4}	1.01×10^{-3}	-2.21×10^{-3}	1.01×10^{-5}	1.01×10^{-5}	1.01×10^{-5}
z_2	1×10^{-3}	6.02×10^{-2}	4.16×10^{-3}	0	0	6.02×10^{-4}
z_1	1×10^{-3}	2.63×10^{-3}	1.18×10^{-2}	0	0	2.63×10^{-5}

TABLE IV. Trilinear Higgs Yukawa couplings in the E₆SSM benchmarks. The couplings λ_{ijk} come from the terms $\lambda_{ijk}\hat{S}_i\hat{H}_{d_j}\hat{H}_{u_k}$ in the superpotential. Here $\lambda_{333} = \lambda$, $\lambda_{3\alpha\beta} = \lambda_{\alpha\beta}$, $\lambda_{\alpha3\beta} = f_{d\alpha\beta}$, $\lambda_{\alpha\beta3} = f_{u\alpha\beta}$, $\lambda_{33\alpha} = x_{d\alpha}$, $\lambda_{3\alpha3} = x_{u\alpha}$, and $\lambda_{\alpha33} = z_\alpha$.

at the electro-weak scale. One should note that we use the notation of the physical gluino mass, $m_{\tilde{g}}$ (MGo) instead of M_3 . The soft trilinear coupling A_λ associated with the SH_uH_d -term is exchanged for the pseudo-scalar Higgs mass M_A .

The details and notations of the CalcHEP model E6SSM-12.02 described above can be found in Appendix B and the model files are accessible from the High Energy Physics Model DataBase (HEPMDB)[30].

IV. GLUINO PRODUCTION AND DECAYS IN THE MSSM AND E₆SSM

The most important processes for supersymmetry searches at hadron colliders are the production of gluinos and squarks, provided that they are not much heavier than charginos and neutralinos. In this paper we consider the case where all of the squarks are heavier than the gluino, which is motivated by the GUT constrained E₆SSM as discussed in section II E, which makes the pair-production of gluinos the most attractive process for E₆SSM search and discovery.

A. Production cross-sections

The tree-level cross section for gluino pair-production at the LHC at 7, 8, and 14 TeV is shown as a function of the gluino mass in Fig. 5. The CTEQ6LL [31] PDFs are used and the cross section is evaluated at the QCD scales $Q = \sqrt{s}$ and $Q = m_{\tilde{g}}$ ⁴.

In Fig. 5 one can see a large scale dependence of the cross section due to the uncertainty in the leading order calculation, which is substantially reduced at NLO level [32–35]. At $Q = m_{\tilde{g}}$, for which the cross section is about 50% larger than at $Q = \sqrt{s}$ at tree level, the product of NLO and NLL K-factors is in the 2.5–5 range for $\sqrt{s} = 7$ TeV for the 500–1500 GeV mass range [35]. To be on the conservative side we use LO cross sections evaluated at $Q = m_{\tilde{g}}$ in our analysis. For our benchmarks with a gluino mass of 800 GeV, the production cross sections are 20.6 fb, 47.5 fb, and 839 fb for the $\sqrt{s} = 7, 8$ and 14 TeV respectively. So, at the present $\sqrt{s} = 8$ TeV LHC energy and expected integrated luminosity of 20 fb⁻¹ by the end of 2012 about 1000 gluino pairs would have been produced.

⁴ Both renormalisation and factorisation scales were chosen to be equal.

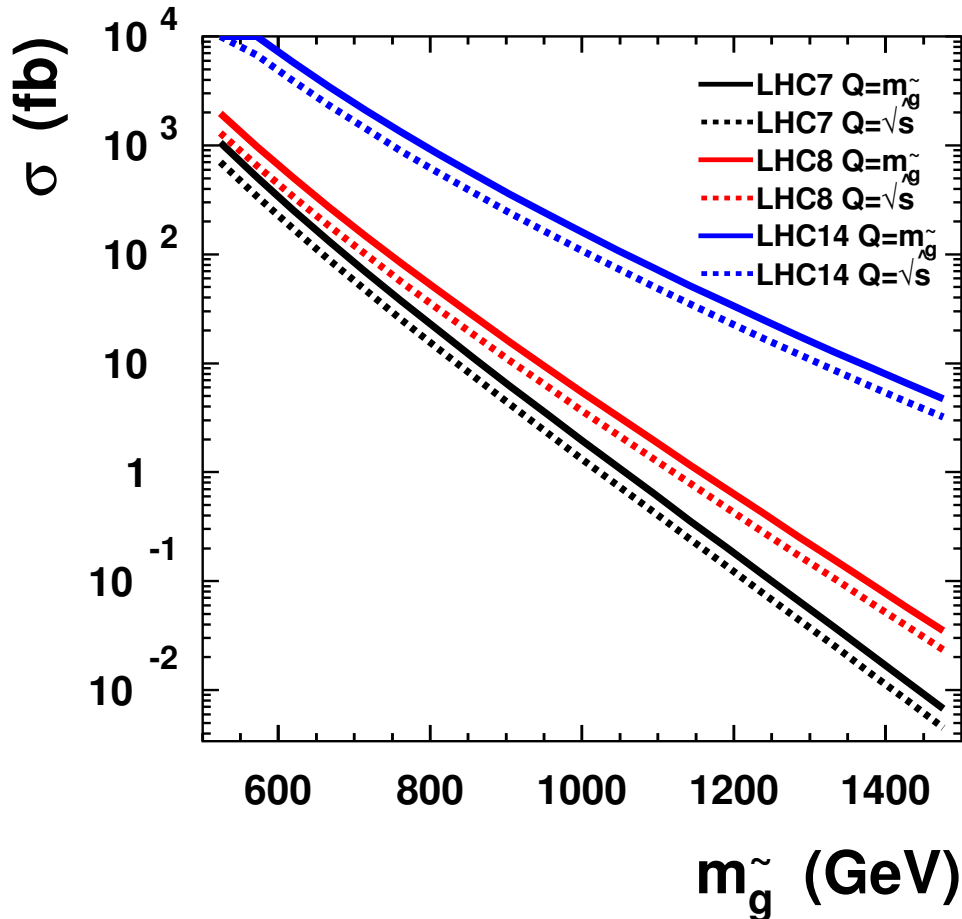


FIG. 5. The tree-level cross section for gluino pair production as a function of the gluino mass, $m_{\tilde{g}}$. The solid (or dashed) lines represent, from bottom to top, the LHC at 7 TeV (black), 8 TeV (red), and 14 TeV (blue). The CTEQ6LL set is used for PDFs. The QCD scale, Q , is set to the gluino mass, $Q = m_{\tilde{g}}$, for the solid lines and to the centre of mass energy, $Q = \sqrt{s}$, for the dashed lines. The scale dependence of the cross section is an effect of the uncertainty of the leading order calculation. Including NLO corrections is known to bring up the cross section by at least a factor 2 [32], so we are underestimating the production rate for gluinos slightly with this leading order calculation.

B. Signatures and distributions

Since the E_6 SSM introduces new neutralinos, naturally lighter than the MSSM-like LSP, the gluino decay chains will be longer than in the MSSM in general. This is confirmed and illustrated by the parameter scans in Fig. 1 and the benchmarks defined in Tab. III. In order to study the LHC phenomenology of gluino cascade decays of the E_6 SSM, and the MSSM for comparison, we have performed Monte Carlo analyses using the CalcHEP [36] package with CTEQ6LL [31] PDFs. With the exception of the multi-jet analysis in section IV D 1, we restrict ourselves to a parton-level analysis. We do however take into account a realistic electromagnetic energy resolution, given by $0.15/\sqrt{E(\text{GeV})}$, typical for the ATLAS and CMS detectors, as well as their typical hadronic energy resolution of $0.5/\sqrt{E(\text{GeV})}$ and perform the respective Gaussian smearing for leptons and quarks. We define leptons (jets) by requiring $p_T > 10$ GeV (20 GeV) and $|\eta| < 2.5$ (4.5) and a lepton isolation of $\Delta R(\text{lepton}, \text{jet}) > 0.5$.

The longer decay chains of gluinos lead to less missing momentum, p_T^{miss} , and larger effective mass $M_{\text{eff}} = p_T^{\text{miss}} + \sum_{\text{visible}} |p_T^{\text{visible}}|$, as measured in the detector as one can see in Fig. 6 which presents the respective distributions for our main benchmarks (MSSM and E_6 SSM-I). Although the p_T^{miss} distribution is quite different, one should note that

the effective mass distribution is not significantly different between the models. This happens because the effect from the suppressed missing momentum in the case of the E_6 SSM is partially canceled by the effect of the increase of visible momentum, due to the longer gluino cascade decay. There is a slight overall increase of the effective mass due to the fact that visible momenta are added up as magnitudes while the missing momentum is a vectorial sum. The reduced amount of missing transverse momentum in the E_6 SSM makes it less discoverable, compared to the MSSM, in typical SUSY searches which focus on all-hadronic events with large missing momentum.

Another important feature of the long decay chains of the E_6 SSM is the increase in lepton as well as jet multiplicity, as shown in Fig. 7, again for the benchmarks MSSM and E_6 SSM-I. This feature allows us to rely on multi-lepton requirements for background reduction rather than cuts on missing energy. There is a significant loss of statistics by using this strategy, however it turns out to be a very important channel for discovery of gluinos with long decay chains and indeed a channel in which the E_6 SSM is largely dominant compared to the MSSM. This makes the multi-lepton channels essential for distinguishing the models.

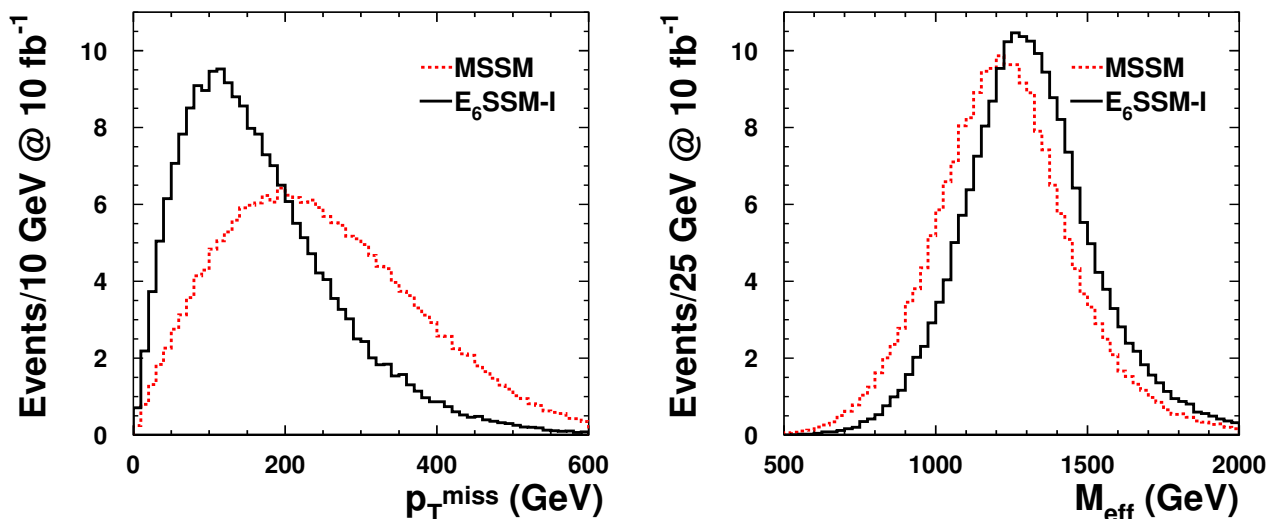


FIG. 6. Missing transverse momentum (left) and the effective mass (right) before cuts for the MSSM and E_6 SSM-I benchmark with $m_{\tilde{g}} = 800$ GeV at $\sqrt{s} = 7$ TeV. The E_6 SSM predicts significantly less missing transverse momentum and slightly larger effective mass compared to the MSSM. The longer gluino decay chains of the E_6 SSM, with a lighter LSP in the end, provide less missing and more visible transverse momentum. The effective mass does not distinguish the features of these models since it is a sum of visible and missing transverse momenta.

C. Searches at $\sqrt{s} = 7$ TeV LHC

There has not been any indications of SUSY from the LHC during its run at $\sqrt{s} = 7$ TeV. We have investigated different SUSY search channels at this energy to understand the status of our benchmarks and what limits can be put on the E_6 SSM and which channels we expect to be the most favourable for discovery and distinguishing the models. We compare our signals with published backgrounds used by CMS and ATLAS at this energy. We have scaled all the channels to an integrated luminosity of 10 fb^{-1} for comparison, which is approximately the amount of 7 TeV data acquired by the two experiments. Benchmarks with an 800 GeV gluino mass are considered here.

1. 0 leptons

The long gluino cascade decays with less missing momentum would be less visible in the main SUSY searches based on jets and missing energy (see e.g. [2] and [37]) which provide the best statistics and strongest exclusions for MSSM. In these searches the E_6 SSM parameter space is less constrained as compared to the MSSM and the acquired

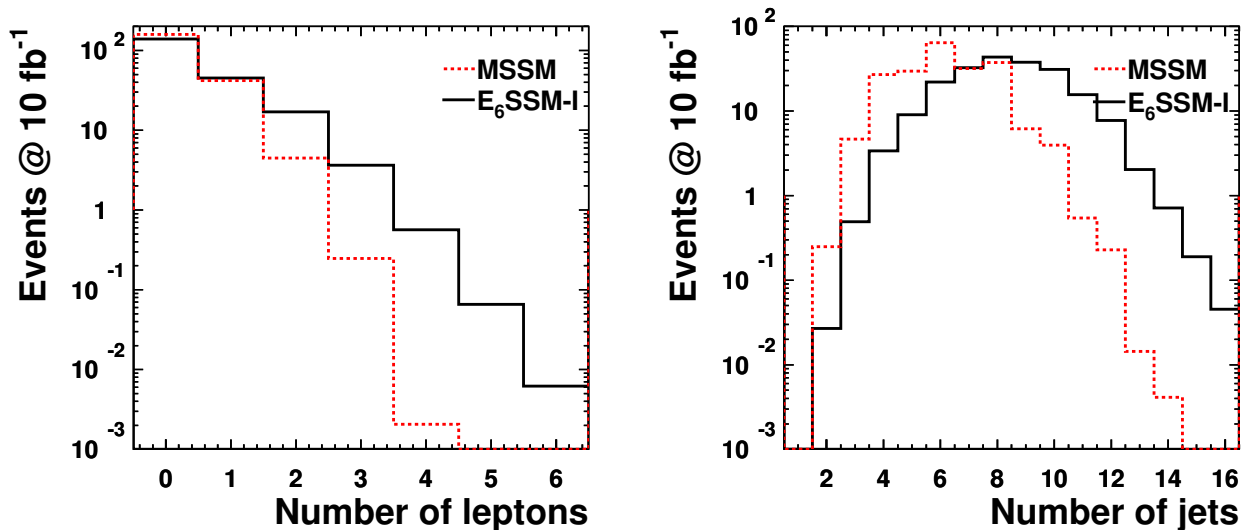


FIG. 7. Lepton multiplicity (left) and jet multiplicity (right), requiring $p_T > 10$ GeV, $|\eta| < 2.5$, and $\Delta R(\text{lepton}, \text{jet}) > 0.5$ for leptons and $p_T > 20$ GeV and $|\eta| < 4.5$ for jets. The benchmarks considered are the MSSM and $E_6\text{SSM-I}$ as presented in Tab. III with $m_{\tilde{g}} = 800$ GeV. The LHC setup is used with $\sqrt{s} = 7$ TeV and normalised to 10 fb^{-1} of integrated luminosity. Due to the longer gluino decay chains of the $E_6\text{SSM}$ it predicts many more visible particles in collider experiments, both leptons and jets. This suggests that searches for $E_6\text{SSM}$ gluinos should be more favourable in multi-lepton and multi-jet searches.

exclusions do not hold for this model. The main reason for this is the hard cuts on missing energy and its ratio to the effective mass since the distributions for these variables are significantly different for MSSM versus $E_6\text{SSM}$ as we demonstrate here.

The effective mass distribution for our benchmarks for an 800 GeV gluino mass is plotted on the top of the backgrounds from ATLAS and CMS in Figs. 8(a) and 8(b) after all cuts have been applied except for the final selection cut on the effective mass itself. The signal from $E_6\text{SSM}$ is suppressed as compared to the MSSM and, more importantly, both benchmarks are well below the background, illustrating the difficulty of discovering SUSY at the 7 TeV LHC in the case where the gluino mass is around 800 GeV, assuming the squarks to be much heavier.

Even though the 0-lepton signature with a jet multiplicity of about four is not favoured for $E_6\text{SSM}$ hunting, the 0-lepton signature for this model could be still interesting for the cases of larger jet-multiplicity. For multi-jet channels, analyses beyond the parton level are essential. We discuss this in detail for the case of $\sqrt{s} = 8$ TeV in section IV D 1 where we perform one example of a beyond-the-parton level analysis. Apart from this, we restrict ourselves here by the parton level analysis and in particular we shall focus on the tri-lepton signature.

2. 1–2 leptons

The selection of events with leptons provides easy triggering and efficient background suppression at the cost of worse statistics. To exemplify this we compare the signal distributions for the benchmarks versus the backgrounds for two ATLAS searches, a single lepton search in Fig. 8(c) and a two same-sign lepton search in Fig. 8(d). One can see that the signal-to-background ratio is better in these leptonic searches compared to the all-hadronic searches. In the effective mass distribution of the 1 muon channel from ATLAS’s 1 lepton plus 4 jets search shown in Fig. 8(c) one can see that the signal level is not extremely far below the background level in the high effective mass region. The $E_6\text{SSM}$ signal is still suppressed as compared to the MSSM in this one lepton search, however, considering the p_T^{miss} distribution for the two same-sign lepton search by ATLAS in Fig. 8(d), one sees how the $E_6\text{SSM}$ signal overtakes the MSSM benchmark’s by requiring one more lepton. This is due to the fact that two same-sign leptons in the final state become more likely in the $E_6\text{SSM}$ than in the MSSM, simply because it predicts more leptons in general. Even though the $E_6\text{SSM}$ signal has got stronger than the MSSM signal in this 2SS channel compared to the one lepton channel, the signal-to-background ratio now looks worse. This is because the choice of using the missing momentum instead

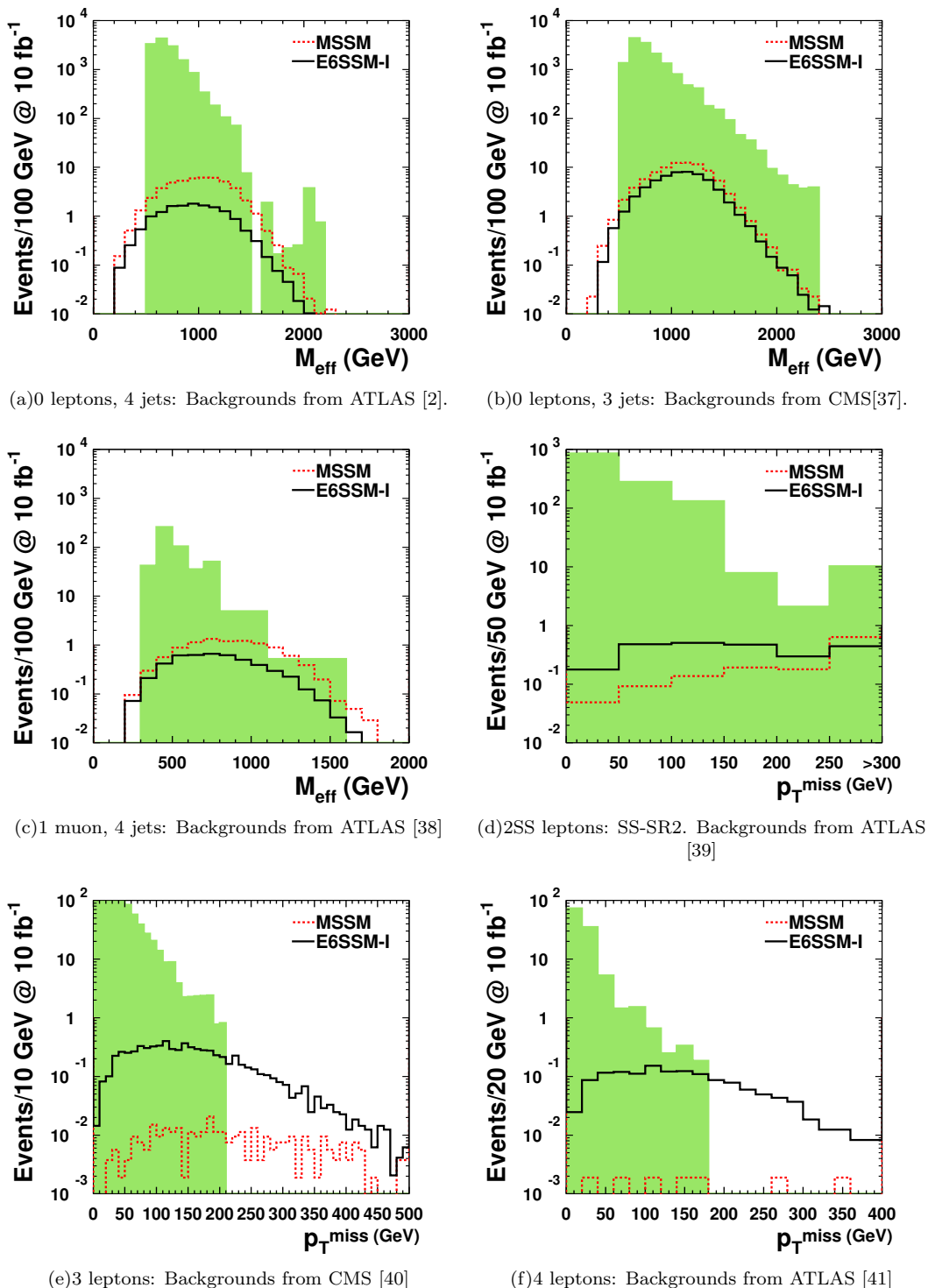


FIG. 8. Distributions for published 0–4 lepton searches at 7 TeV, scaled to 10 fb^{-1} for comparison. The signal contributions from the MSSM and $E_6\text{SSM-I}$ benchmarks with $m_{\tilde{g}} = 800 \text{ GeV}$ are plotted on top of published backgrounds. The distributions shown are after all cuts except the final selection cut on the plotted distribution. 0 lepton searches (with jets ≤ 4) give bad background suppression and favour MSSM. Requiring two or more leptons makes MSSM more suppressed. For multi-lepton searches the signal to background ratio for the $E_6\text{SSM}$ is better but the signal statistics is low.

of the effective mass as the variable to define the signal region is not favourable for the $E_6\text{SSM}$ since the respective signal is very vulnerable to hard cuts on this variable. Also for higher multiplicity searches, using the effective mass

to define the signal region allows for the signal-to-background ratio to be improved as we will show below.

3. 3-4 leptons

Requiring additional leptons makes the statistics even worse, but it allows the signal to appear above the background enough to allow a reasonable signal significance in order to test the models under study. Comparison of the benchmark signals with the background from a 3 lepton search by CMS is shown in Fig. 8(e) and from a 4 lepton search by ATLAS in Fig. 8(f). The three lepton channel defined by the cuts

$$\begin{aligned} p_T(l_1) &> 20 \text{ GeV} \\ p_T(l_2) &> 10 \text{ GeV} \\ p_T(l_3) &> 10 \text{ GeV} \end{aligned} \tag{IV.1}$$

where $l = \mu$ or e with $|\eta| < 2.5$, and $\Delta R(\text{lepton}, \text{jet}) > 0.5$, seems promising, showing a possible excess in the high missing transverse momentum region. The background used by CMS is not evaluated for large enough missing transverse momentum however. To explore the large missing transverse momentum region and to expand the analysis further we have produced backgrounds for this channel, including several processes, using `CalcHEP`.

The dominant backgrounds come from ZWj and $t\bar{t}V$. Other important contributions come from ZW and $t\bar{t}$. We also considered backgrounds such as $ZWjj$, ZZ and ZZZ which we found to be subleading. Our background predictions at $\sqrt{s} = 7$ TeV agree well with backgrounds used in the multi-lepton searches by CMS [40] and ATLAS [41]. They only major difference is in the very low end of the p_T^{miss} distribution where the `CalcHEP` generated backgrounds are suppressed.

This difference in the transverse missing momentum distribution between our results and the results from the full detector simulation occurs because we do not simulate any source of instrumental missing energy in our analysis. However, this difference does not affect our results since we are not using missing p_T information directly, similar to approach of [42], and, moreover, this difference effectively vanishes after the cut is applied on the effective mass variable as used at last stage of our analysis.

We would like to stress that parton level analysis are quite accurate to the tri-lepton signature we study in this paper. Signatures with lower lepton multiplicity require considering QCD backgrounds from jets faking leptons and instrumental defects which could affect the low p_T^{miss} region. This background is difficult to take into account at the parton-level event generator and even at the level fast detector simulation. Therefore analysis of signatures with the lepton multiplicities below three are outside of the scope of our paper. In case we compare signal versus background for these signatures for the illustration purposes we chose to rely on published backgrounds for those channels in this paper.

The result for the p_T^{miss} distribution is shown in Fig. 9(a). One can see that the $E_6\text{SSM}$ signal is now at the same level as the background and maybe a little higher for large p_T^{miss} . If one instead considers the effective mass as a selection variable for the three lepton channel, the situation looks much more promising, at least for the $E_6\text{SSM}$. This can be seen from the effective mass distribution presented in Fig. 9(b). CMS has not been using the effective mass to define the signal region for this channel but uses the missing transverse energy and the hadronic transverse energy instead. Our way of defining the signal region by the effective mass is on the other hand much closer to the way presented by ATLAS in [41] or as suggested in [42]. A cut on M_{eff} at 950 GeV gives $S = 11.5$ signal events for the 800 GeV gluino mass $E_6\text{SSM-I}$ benchmark and $B = 0.4$ background events, providing an expected 5.7σ excess at 10 fb^{-1} , using the definition of statistical significance $S_{12} = 2(\sqrt{S+B} - \sqrt{B})$ valid for small statistics [43, 44].

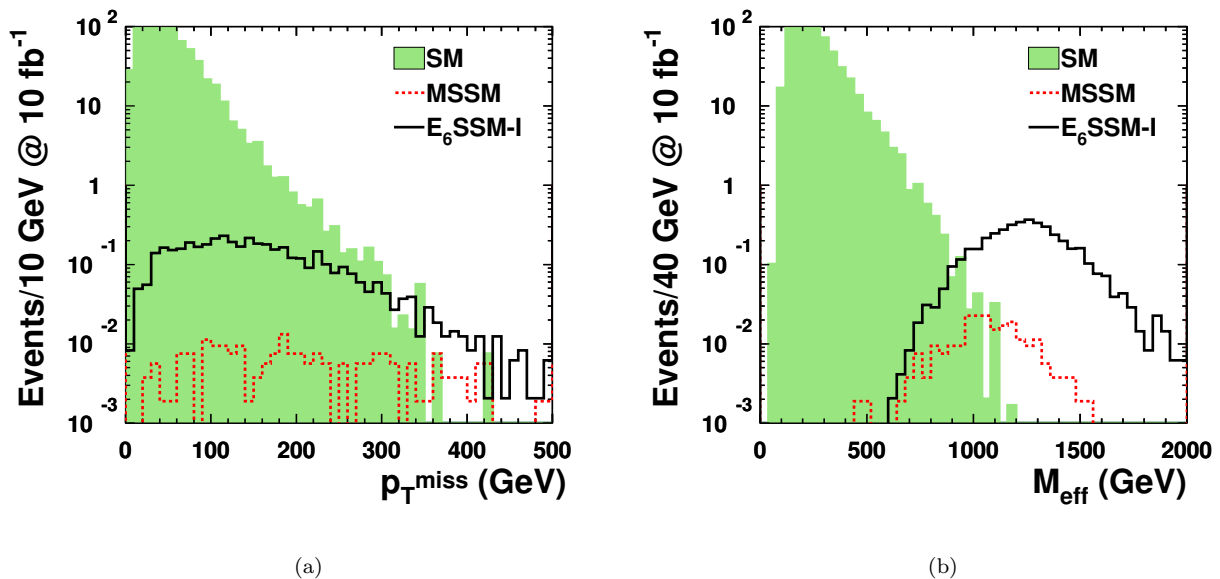


FIG. 9. Distributions for p_T^{miss} (a) and M_{eff} (b) at the LHC with 10 fb^{-1} at $\sqrt{s} = 7 \text{ TeV}$ after requiring at least three leptons. The benchmarks both have a gluino mass $m_{\tilde{g}} = 800 \text{ GeV}$. Backgrounds have been generated by CalcHEP and agree well with published ones such the ones by CMS, shown in Fig. 8(e). The $E_6\text{SSM-I}$ benchmark is shown to present a signal larger than the background for large missing momentum (a) even though it is a model that predicts quite small amounts of missing momentum. The signal presents itself more strongly in the effective mass variable where there is no need for a cut on the missing transverse momentum.

D. Searches at $\sqrt{s} = 8 \text{ TeV}$ LHC

1. 6 jets

Since the multi-jet channels could provide good prospects of discovery of and differentiation between benchmarks we investigate the effect of the cuts,

$$\begin{aligned}
 E_T^{\text{miss}} &> 160 \text{ GeV} \\
 p_T(j_1) &> 130 \text{ GeV} \\
 p_T(j_2) &> 60 \text{ GeV} \\
 p_T(j_3) &> 60 \text{ GeV} \\
 p_T(j_4) &> 60 \text{ GeV} \\
 p_T(j_5) &> 60 \text{ GeV} \\
 p_T(j_6) &> 60 \text{ GeV} \\
 \Delta\phi(\text{jet}, p_T^{\text{miss}})_{\text{min}} &> 0.4(i = \{1, 2, 3\}), 0.2(p_T > 40 \text{ GeV jets}) \\
 E_T^{\text{miss}}/m_{\text{eff}} &> 0.25(6j) \\
 m_{\text{eff}} &> 1300 \text{ GeV},
 \end{aligned} \tag{IV.2}$$

used by ATLAS [45] for 6-jets analysis applied to our benchmarks. To perform this kind of multi-jet analysis we are forced to go beyond our parton-level analysis. The need for a more dedicated analysis, with hadronisation and detector effects, comes mainly from the importance of initial and final state radiation that plays an important role when requiring more than four jets in the gluino decays. This is because the first four jets are well approximated by our parton level analysis since they typically are the ones that originate straight from the gluino decay. To generate the events at the level of fast detector simulation we fed events from CalcHEP to the PGS [46] package. We also compare the signal from the MSSM and $E_6\text{SSM}$ with an mSUGRA point which is excluded, but very close to the limit. The result for the effective mass distribution for the signals before and after cuts are shown in Fig. 10.

Our result, produced with CalcHEP and PGS, is in good agreement with the ATLAS result and is consistent with the experimental data.

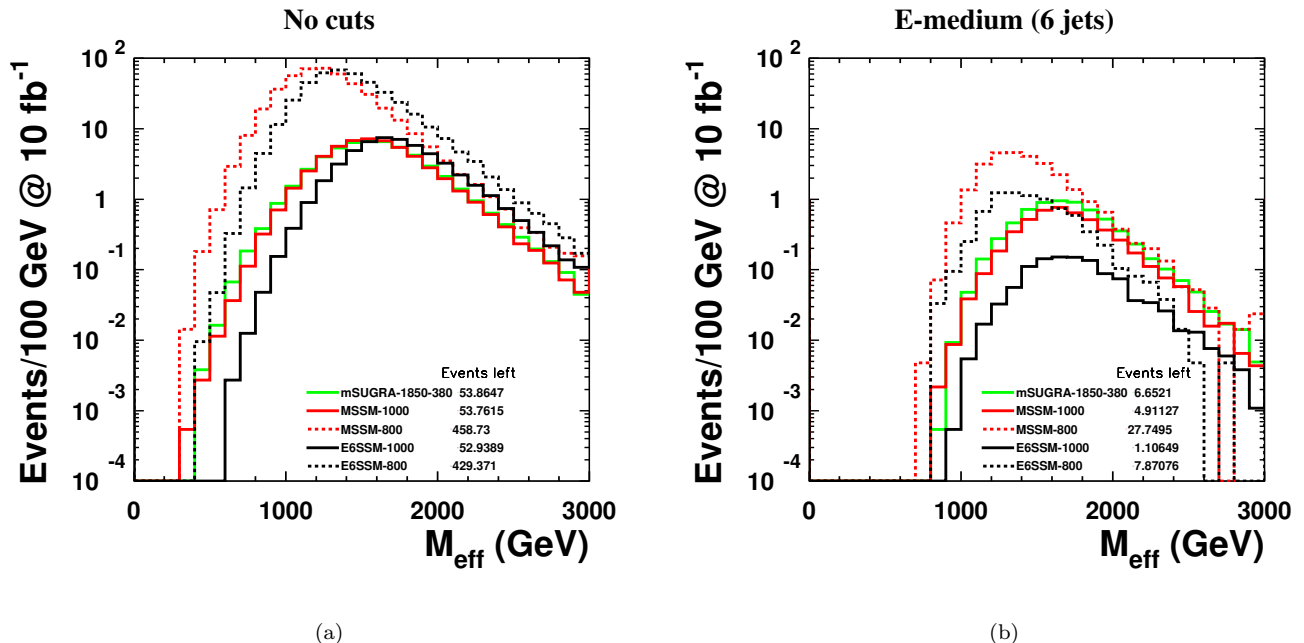


FIG. 10. Comparison between mSUGRA, MSSM, and E₆SSM benchmarks in the 6 jet channel, E-medium, used by ATLAS [45]. The effective mass distribution for the gluino signal are plotted before (a) and after (b) cuts at $\sqrt{s} = 8$ TeV and 10 fb^{-1} of integrated luminosity. The events left after the last signal region cut on the effective mass, $M_{\text{eff}} > 1300$ GeV, are given in Tab. V. The benchmarks with solid lines all have a gluino mass of 1 TeV while the benchmarks with dashed lines have a gluino mass of 800 GeV. After cuts (b) the E₆SSM benchmark with an 800 GeV gluino mass has a distribution not very different from the mSUGRA point with a 1 TeV gluino mass.

Our analysis shows that, also in the multi-jet channels, the E₆SSM will be suppressed compared to the MSSM and mSUGRA models, mostly because of its small missing transverse momentum. The larger jet multiplicity of the E₆SSM at the parton level turns to be not such a great discriminator between two models, at least for this signature, because the initial and final state radiation allows most of the signal from the MSSM model to pass the 6-jets selection requirement. Even though it might still be a good discovery channel for different selection/analysis for the E₆SSM, we note that, for the current selection, the E₆SSM signal from an 800 GeV gluino is about at the same level as the signal from the mSUGRA model with a 1 TeV gluino. This is the very important point we would like to convey in this paper: the MSSM limits are not quite applicable to the E₆SSM, for example the gluino mass limit could easily differ by about 200 GeV between two models in the heavy squark limit as we demonstrate above. Therefore the status of the E₆SSM is quite different even from generic MSSM one for the current LHC analysis, which needs to be tuned in order to explore E₆SSM parameter space.

	$m_{\tilde{g}}/\text{TeV}$	Events
mSUGRA (1850,380)	1	6.18
	0.8	18.16
MSSM	1	5.59
	0.8	18.16
E ₆ SSM	1	1.05
	0.8	5.58

TABLE V. The events left at 8 TeV and 10 fb^{-1} for benchmarks from three models after the E-medium set of cuts, including the final cut on the effective mass, $M_{\text{eff}} > 1300$ GeV. Here the E₆SSM benchmark with a 800 GeV gluino mass is left with less events than the mSUGRA benchmark with a 1 TeV gluino mass.

2. 3 leptons

Performing the same analysis for the promising 3 lepton channel at the LHC with $\sqrt{s} = 8$ TeV as was done for the case with $\sqrt{s} = 7$ TeV we are able to calculate the discovery prospects for our benchmarks. Again, the 3 lepton signature is defined by the cuts in IV.1. In Fig. 11 the effective mass distributions are plotted for our benchmarks and SM backgrounds for 20 fb^{-1} of integrated luminosity. The different plots show how the effective mass distributions change for the benchmarks if the gluino mass is varied.

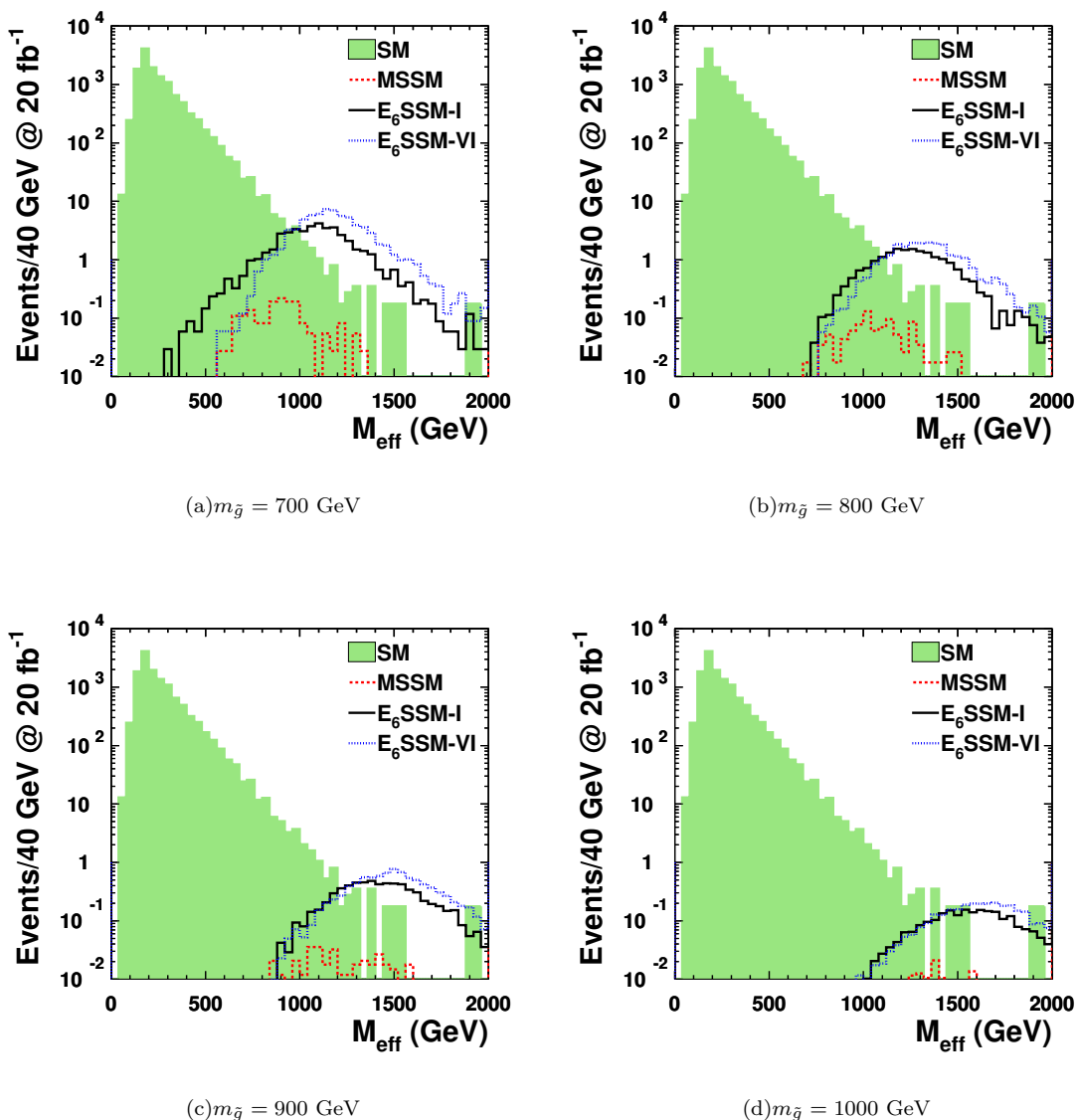


FIG. 11. Plots of M_{eff} after requiring at least 3 leptons at LHC at $\sqrt{s} = 8$ TeV. The integrated luminosity is taken to be 20 fb^{-1} . The different subfigures show the signal distributions for the MSSM, $E_6\text{SSM-I}$, and $E_6\text{SSM-VI}$ benchmarks for different values of the gluino mass. The $E_6\text{SSM-VI}$ benchmark is similar to $E_6\text{SSM-I}$, but the lighter LSP mass, and thus larger mass gap between it and the bino-like neutralino, causes the signal to be stronger since higher p_T leptons are more likely to be produced. The distributions for gluino masses of 700 GeV (a), 800 GeV (b), 900 GeV (c), and 1000 GeV (d) show that the signal to background ratio is not affected much as the gluino mass increases, but the statistics become bad since the cross section gets small.

In these plots we have included another benchmark, $E_6\text{SSM-VI}$, for comparison with the $E_6\text{SSM-I}$ and MSSM benchmarks. This benchmark gives a signal slightly above that of the $E_6\text{SSM-I}$. This is because the $E_6\text{SSM-VI}$

benchmark has a long gluino decay chain with an even less compact spectrum. The larger mass difference between the MSSM-like lightest neutralino and the inert singlinos implies that higher p_T leptons can be radiated from that step in the decay chain. This causes an increase in the number of leptons surviving the lepton identification cuts.

A final cut, defining the signal region, is made on the effective mass. We let the signal region cut depend on the gluino mass to enhance the expected significance and define it as $M_{\text{eff}} > 1.4m_{\tilde{g}}$.

Using the definition of statistical significance, $S_{12} = 2(\sqrt{S+B} - \sqrt{B})$, valid for small statistics [43, 44], we calculate the expected excess for different gluino masses using our mass dependent signal region cut.

The significance is plotted as a function of the gluino mass in Fig. 12(a) where a K-factor of 3 has been applied to the signal. The expected number of events for the E₆SSM-I and E₆SSM-VI benchmarks with gluino mass $m_{\tilde{g}} = 900$ GeV and the background before and after the final cut on the effective mass ($M_{\text{eff}} > 1.4m_{\tilde{g}} = 1260$ GeV) are presented in Tab. VI. The table also lists the expected significances with and without a K-factor of 3 for the two benchmarks. The integrated luminosity needed for discovery and exclusion of a particular gluino mass in the E₆SSM in the 3 lepton channel is shown in Fig. 12, where again a K-factor of 3 has been applied to the signal. The plot shows that a 2σ exclusion of gluino masses below 1 TeV is possible with data acquired by ATLAS or CMS at the end of the year 2012. The MSSM benchmark is still well below the background at this stage and is therefore not included in these plots.

	$N_{\text{lep}} \geq 3$	$M_{\text{eff}} > 1.4m_{\tilde{g}}$	$\sigma_{K=1}$	$\sigma_{K=3}$
E ₆ SSM-I	6.72	5.08	2.80	5.88
E ₆ SSM-VI	8.95	7.60	3.71	7.57
BG	8.66×10^3	1.25		

TABLE VI. The expected number of events after the first and second cuts in the 3 lepton analysis for the E₆SSM-I and E₆SSM-VI benchmarks with $m_{\tilde{g}} = 900$ GeV and SM background at 20 fb^{-1} and 8 TeV. Also the significance, based on signal and background events after the second cut, with K-factors of 1 and 3 applied to the signal.

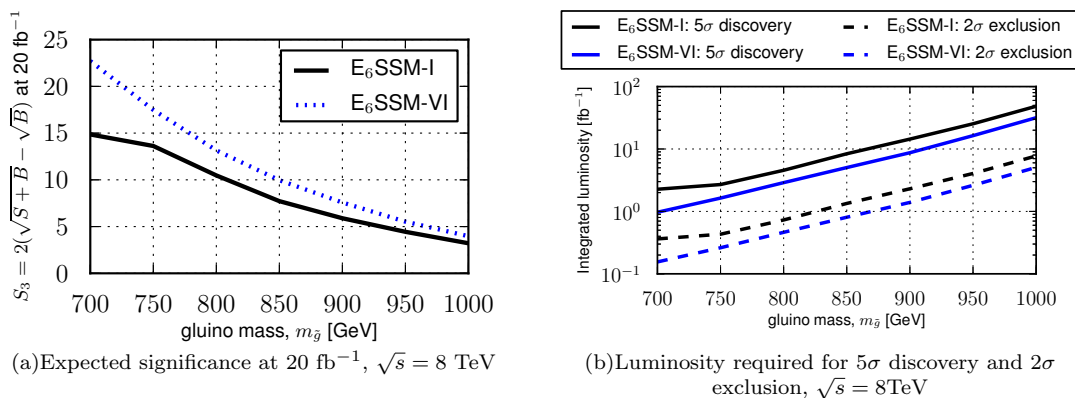


FIG. 12. The gluino mass reach at $\sqrt{s} = 8$ TeV for the three lepton channel. The gluino mass is varied for the benchmarks E₆SSM-I and E₆SSM-VI to estimate the expected significance for different gluino masses. The significance is calculated with the events remaining after a selection cut requiring $M_{\text{eff}} > 1.4m_{\tilde{g}}$. A K-factor of 3 has been applied to the signal. The E₆SSM-VI benchmark (shown in blue) is more accessible for exclusion or discovery than benchmark E₆SSM-I since it has a bigger mass gap between the bino-like and inert-singlino-like neutralinos, providing higher p_T leptons.

E. 3 lepton searches at $\sqrt{s} = 14$ TeV LHC

At higher collider energy the cross section for gluino production increases considerably. This causes both our MSSM and E₆SSM benchmarks to be clearly visible above the background, as can be seen in Fig. 13. The figure shows the effective mass distribution for the MSSM, E₆SSM-I, and E₆SSM-VI benchmarks for different gluino masses in different subfigures, where a requirement of at least three leptons has been applied in the same way as in the 8 TeV analysis. For all gluino masses the E₆SSM-VI benchmark gives the largest signal, just as in the 8 TeV scenario discussed in section IV D 2. The 14 TeV collider at such a large integrated luminosity as 100 fb^{-1} , which is used in Fig. 13, allows for statistics needed for discovery of high mass gluinos. Heavier gluinos would push the effective mass distribution to

higher values where there is essentially no background and where it is just a matter of acquiring enough statistics, but once that is done one expects a very clean signal.

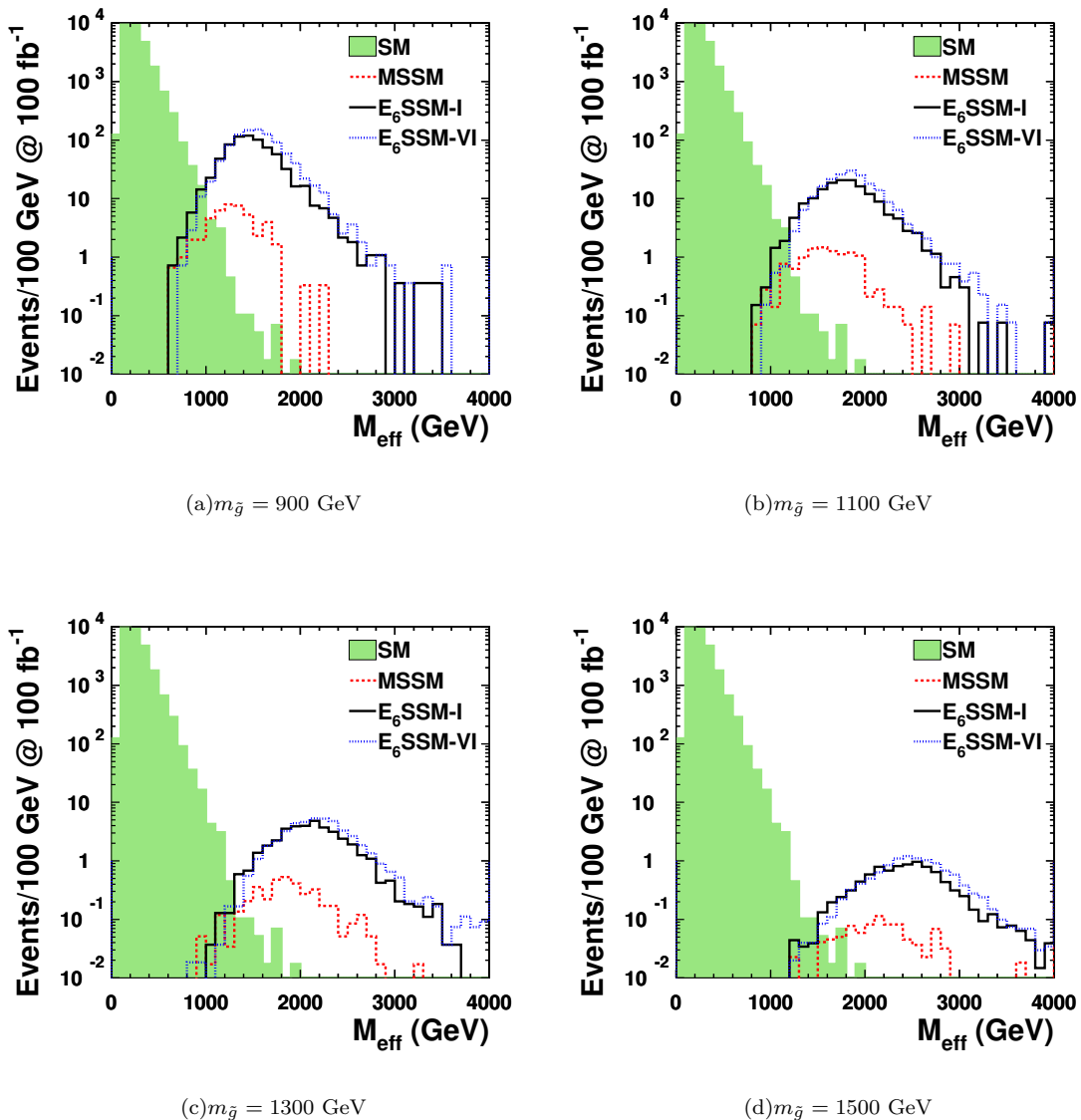


FIG. 13. These plots show the evolution of the effective mass distribution after requiring at least three leptons for the benchmarks MSSM, E_6 SSM-I, and E_6 SSM-VI as the gluino mass changes. In Figure 13(a) the gluino mass is 900 GeV and at this large integrated luminosity of 100 fb^{-1} at $\sqrt{s} = 14$ TeV the MSSM benchmark is almost discoverable. The E_6 SSM benchmarks are both well above the background and clear signals are expected due to the good statistics.

In Fig. 14 the gluino reach for the benchmarks at the 14 TeV collider is presented in the same way as was done for the 8 TeV collider in Fig. 12, again with a K-factor of 3 applied to the signal. The only difference is that the gluino mass dependent cut on the effective mass which defines the signal region is taken to be $M_{\text{eff}} > m_{\tilde{g}}$ instead of $M_{\text{eff}} > 1.4m_{\tilde{g}}$. For the MSSM benchmark, which has become accessible at this energy, one will be able to exclude gluino masses up to ~ 1400 GeV through this channel for an integrated luminosity of 100 fb^{-1} . The expected significance for the MSSM is however about an order of magnitude below the E_6 SSM benchmarks as shown in Fig. 14(a). An order of magnitude difference in significance implies two orders of magnitude difference for the the integrated luminosity required for exclusion of a particular gluino mass, as can be seen in Fig. 14(b). For the E_6 SSM-I and E_6 SSM-VI the 100 fb^{-1} of data at 14 TeV allows not only for exclusion, but potentially for a 5σ discovery for the whole gluino mass range up to 1.5 TeV.

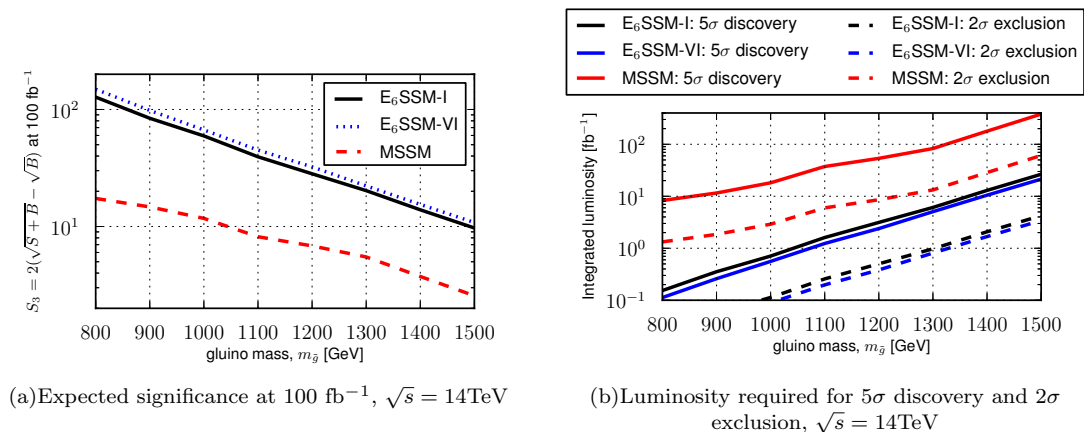


FIG. 14. The gluino mass reach at $\sqrt{s} = 14 \text{ TeV}$ for the three lepton channel. The gluino mass has been varied for the benchmarks E_6 SSM-I, E_6 SSM-VI, and MSSM. The expected significance is calculated using the signal and background events surviving the cut $M_{\text{eff}} > m_{\tilde{g}}$. A K-factor of 3 has also been applied to the signal. Here at the higher collider energy the MSSM benchmark also becomes discoverable through this 3 lepton channel. The E_6 SSM benchmarks are discoverable up to almost a 1500 GeV gluino mass.

It should be stressed once more that the results for the MSSM benchmark are different from other studies since we are not dealing with a GUT constrained model, but an electro-weak scale model and the spectrum is more general. Our study focuses on a specific scenario in which the squarks are two to three times heavier than the gluino. Therefore, typical results obtained in previous multi-lepton analyses for SUSY searches differ from our results. As an example, the three lepton signals derived for the mSUGRA points in [42] are larger than the signals for the benchmarks considered in this paper with the same gluino mass. This is mainly due to the lighter squark masses assumed in that study, giving rise to a larger cross section, but also partly due to the entire assumed spectrum being very different. These differences play a crucial role in providing different p_T distributions for the leptons arising from gluino cascade decays between the different models.

V. CONCLUSIONS

SUSY is an attractive candidate for new BSM physics, but so far it remains elusive at the LHC. A generic prediction of all SUSY models is the gluino, which can be produced with a large cross-section at the LHC due to its colour octet nature. Moreover in many SUSY models it may be the lightest coloured SUSY particle, which could make it the first SUSY particle to be discovered. However the gluino typically decays in cascade decays, via a chain of charginos and neutralinos, emitting jets or leptons at each stage of the decay chain, with the chain ending when the LSP is produced which is typically the lightest neutralino.

In this paper we have discussed the gluino cascade decays in E_6 models, which include matter and Higgs filling out three complete 27 dimensional representations close to the TeV scale. In such models there are three families of Higgs doublets of both H_u and H_d kinds, plus three Higgs SM-singlets of the NMSSM kind S . Only the third family acquire VEVs and the other two families do not and are called inert. All these Higgs states are accompanied by spin-1/2 SUSY partners, the Higgsinos. The extra inert charged and neutral Higgsinos, some of which are necessarily light, will mix with the usual MSSM charginos and neutralinos, yielding extra light states, providing extra links in the gluino cascade decays, and hence extra jets and leptons, with less missing energy.

The extra neutralinos and charginos generically appearing in a large class of E_6 inspired models lead to distinctive signatures from gluino cascade decays in comparison to those from the MSSM. These signatures involve longer decay chains, more visible transverse energy, higher multiplicities of jets and leptons, and less missing transverse energy than in the MSSM. We have studied this effect in gluino cascade decays for the MSSM and E_6 SSM and have shown that it can provide a characteristic and distinctive signature of the model, enabling an early discovery of the E_6 SSM which may be discriminated from the MSSM.

In order to demonstrate this, we have first defined a rather large set of benchmark points within the E_6 SSM. These benchmark points are chosen for the variety of ways in which the inert charginos and neutralinos can appear, and they all are chosen to have a nominal gluino mass of about 800 GeV, although this can be varied while keeping the inert chargino and neutralino masses unchanged. The results discussed below are remarkably robust, and apply to all

of the E_6 benchmark points. These E_6 benchmarks are also compared to an MSSM benchmark which is chosen to have similar conventional (non-inert) chargino and neutralino masses to the E_6 ones, as well as mSUGRA points, in order to verify the model independence of the conclusions.

Given this set of benchmark points, we have then studied gluino pair production and decay at the LHC, first at 7 TeV, then at 8 TeV, and eventually at 14 TeV using a Monte Carlo analysis. We already know that the gluino was not discovered at 7 TeV, which motivates the nominal choice of gluino mass of 800 GeV. For this gluino mass, we have first studied the missing transverse momentum and effective mass distributions for representative benchmark points, and seen that the former has a softer spectrum in the E_6 models when compared to the MSSM, as expected, while the latter has a similar or slightly harder distribution in the effective mass variable. Staying at 7 TeV, we then calculated the lepton and jet multiplicities in E_6 models and showed that they are significantly higher than in the MSSM. This motivated a study of lepton channels with increasing numbers of leptons, and decreasing statistics, where we showed that the 3 lepton channel provided a very good discriminator between the MSSM and the E_6 models, although the statistics are rather too low at 7 TeV.

At 8 TeV we studied the 6 jet channel and showed that, in an effective mass analysis, a 1 TeV MSSM gluino may provide a similar limit to that of an 800 GeV E_6 gluino. Turning to the promising 3 lepton channels at 8 TeV, we find increased statistics and possible observable signals in this channel for a range of gluino masses, which would provide a striking confirmation of E_6 models. We calculate the required integrated luminosity in order to either discover or exclude the E_6 gluino in this channel at 8 TeV. We emphasise again that the MSSM gluino is unobservable in the 3 lepton channel. Finally we have repeated the analysis for the promising 3 lepton channel at 14 TeV and found analogous results for required integrated luminosity to discover or exclude the E_6 gluino there as well.

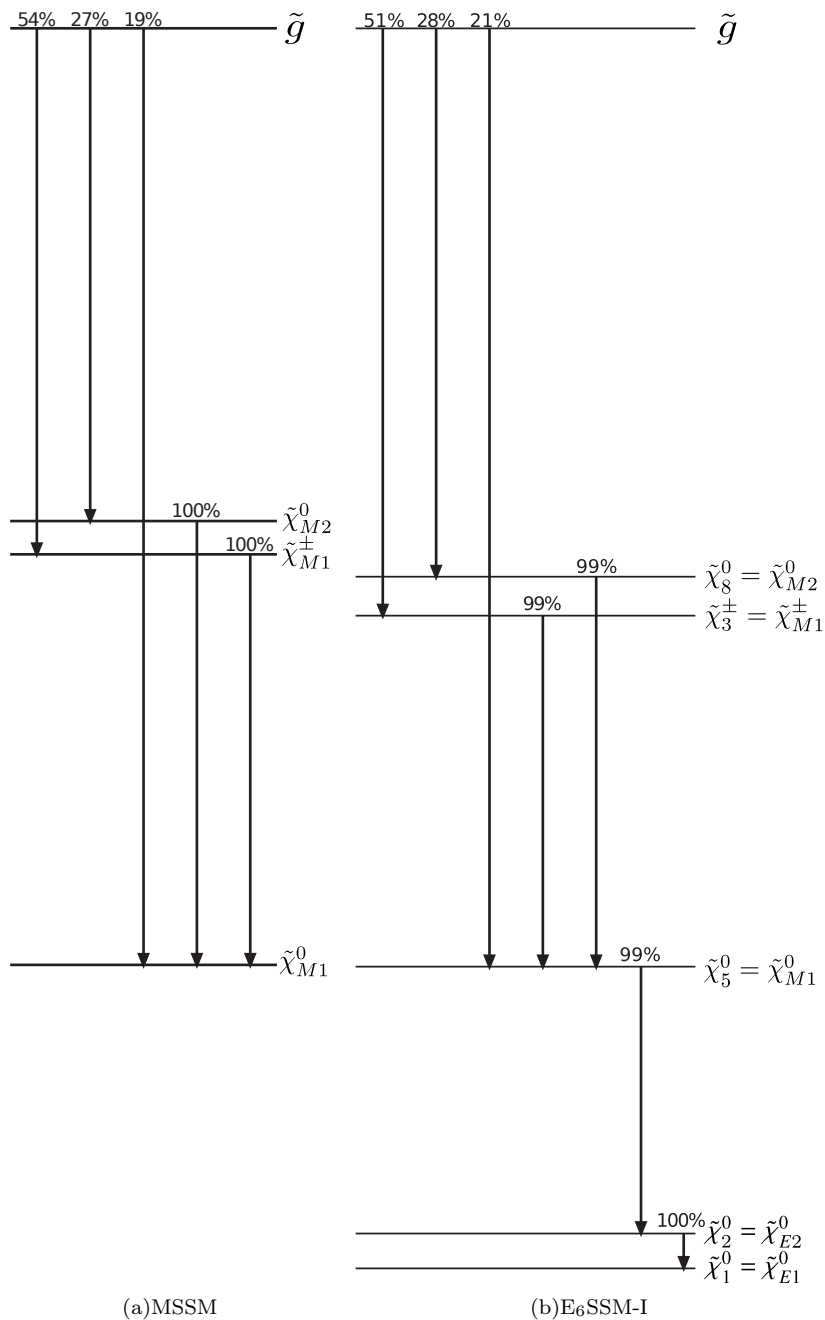
In conclusion, the E_6 inspired models are clearly distinguishable from the MSSM in gluino cascade decays at the LHC with the full data set at 8 TeV, and certainly at 14 TeV, using the three lepton channel that we have proposed. Moreover, the present limits on the gluino mass, for example from a multijet analysis, are weaker (and therefore not applicable) for E_6 models in comparison with the MSSM, due to the longer decay chains with less missing transverse energy that is expected in E_6 models. We emphasise to the LHC experimental groups that the distinctive features present in gluino cascade decays, resulting in different search strategies including the choice of the kinematical variables, such as those discussed here, not only represents a unique footprint of a particular model but also may provide the key to an earlier discovery of supersymmetry.

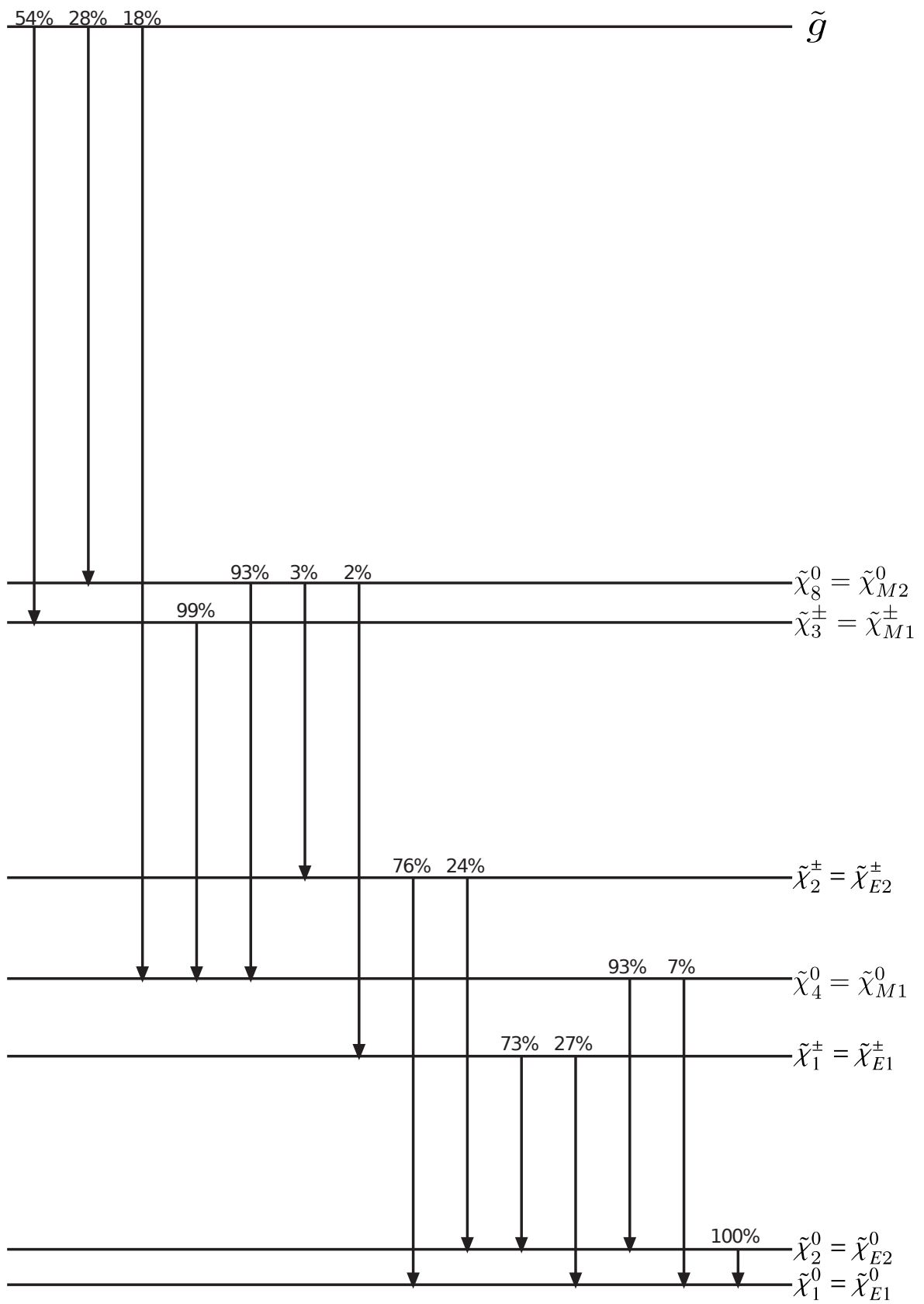
ACKNOWLEDGMENTS

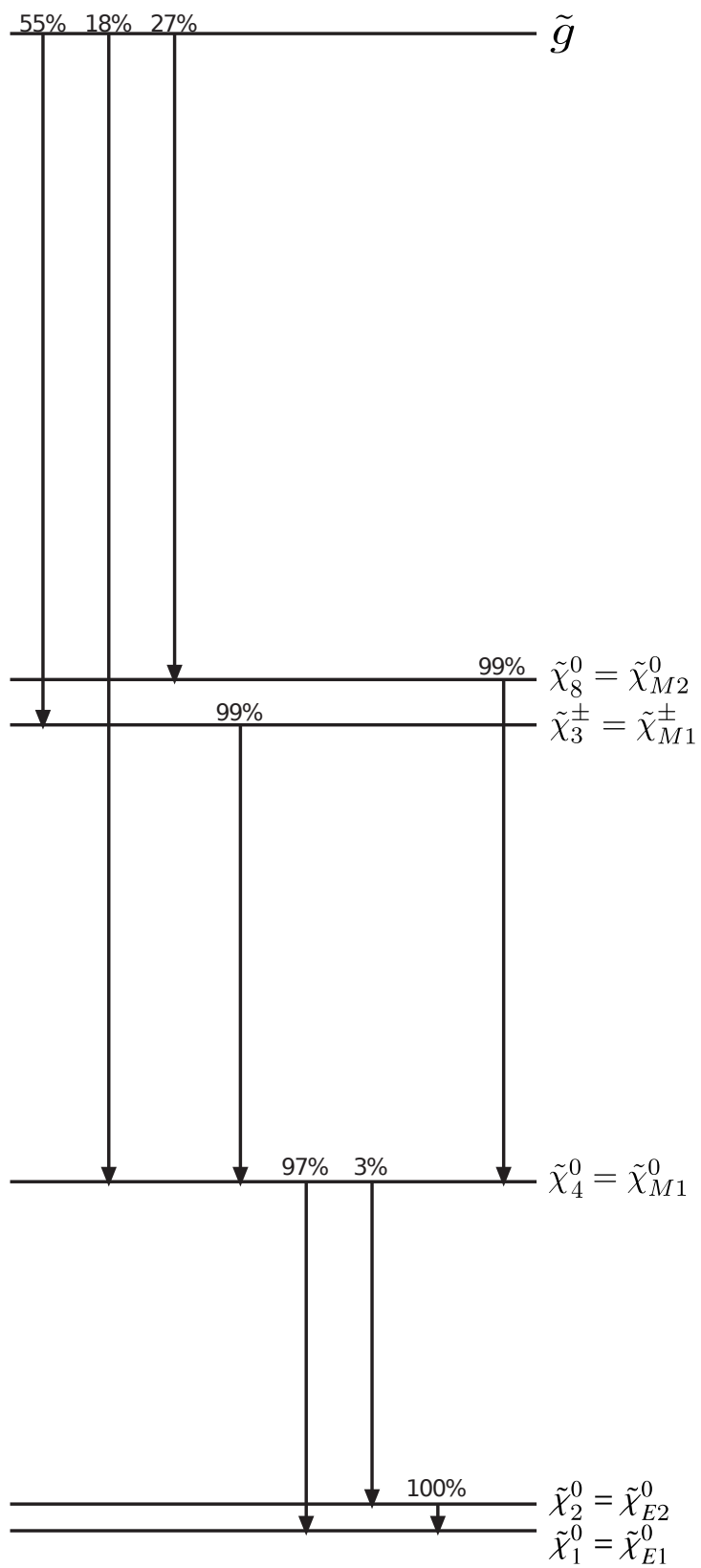
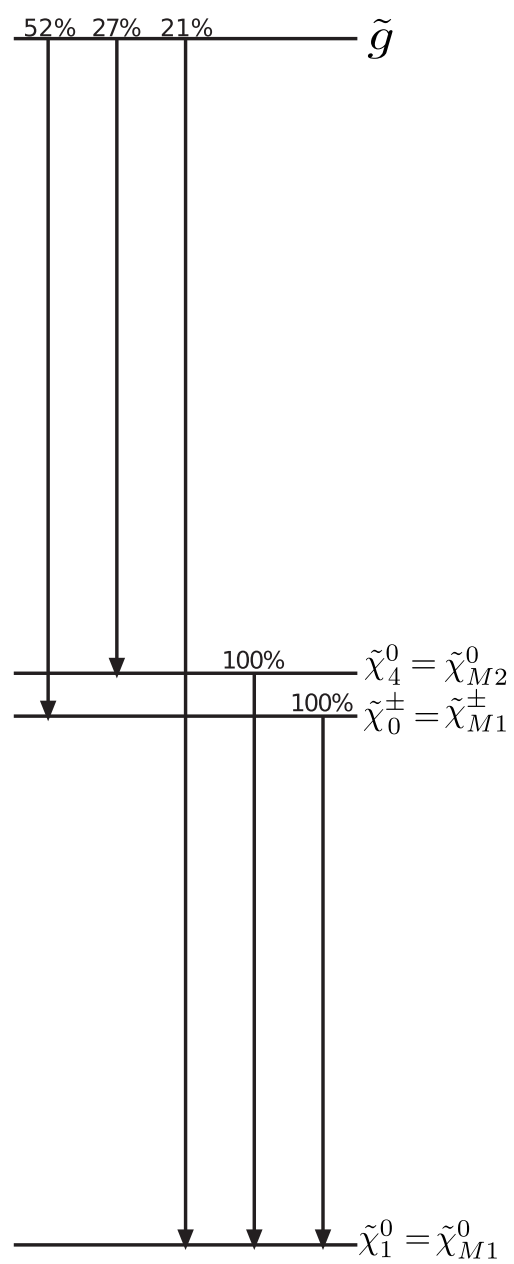
We acknowledge partial support from the STFC Consolidated ST/J000396/1 and EU ITN grants UNILHC 237920 and INVISIBLES 289442. PS thanks the NExT institute and SEPnet for support.

Appendix A: Decay Diagrams for Benchmarks

This section displays the possible gluino decays of each benchmark in a more complete fashion. Horizontal lines representing particle states are separated proportionally to their mass difference. Some exceptions are made where states are closely degenerate, in which case the lines have been separated more. An arrow then connects lines where possible decays occur with the corresponding branching ratio written above. The gluino decays of the MSSM benchmark is shown in Fig. 15(a), E₆SSM-I in Fig. 15(b), E₆SSM-II in Fig. 15(c), E₆SSM-III in Fig. 15(d), E₆SSM-IV in Fig. 15(e), E₆SSM-V in Fig. 15(f) and E₆SSM-VI in Fig. 15(g).



(c)E₆SSM-II

(d)E₆SSM-III(e)E₆SSM-IV

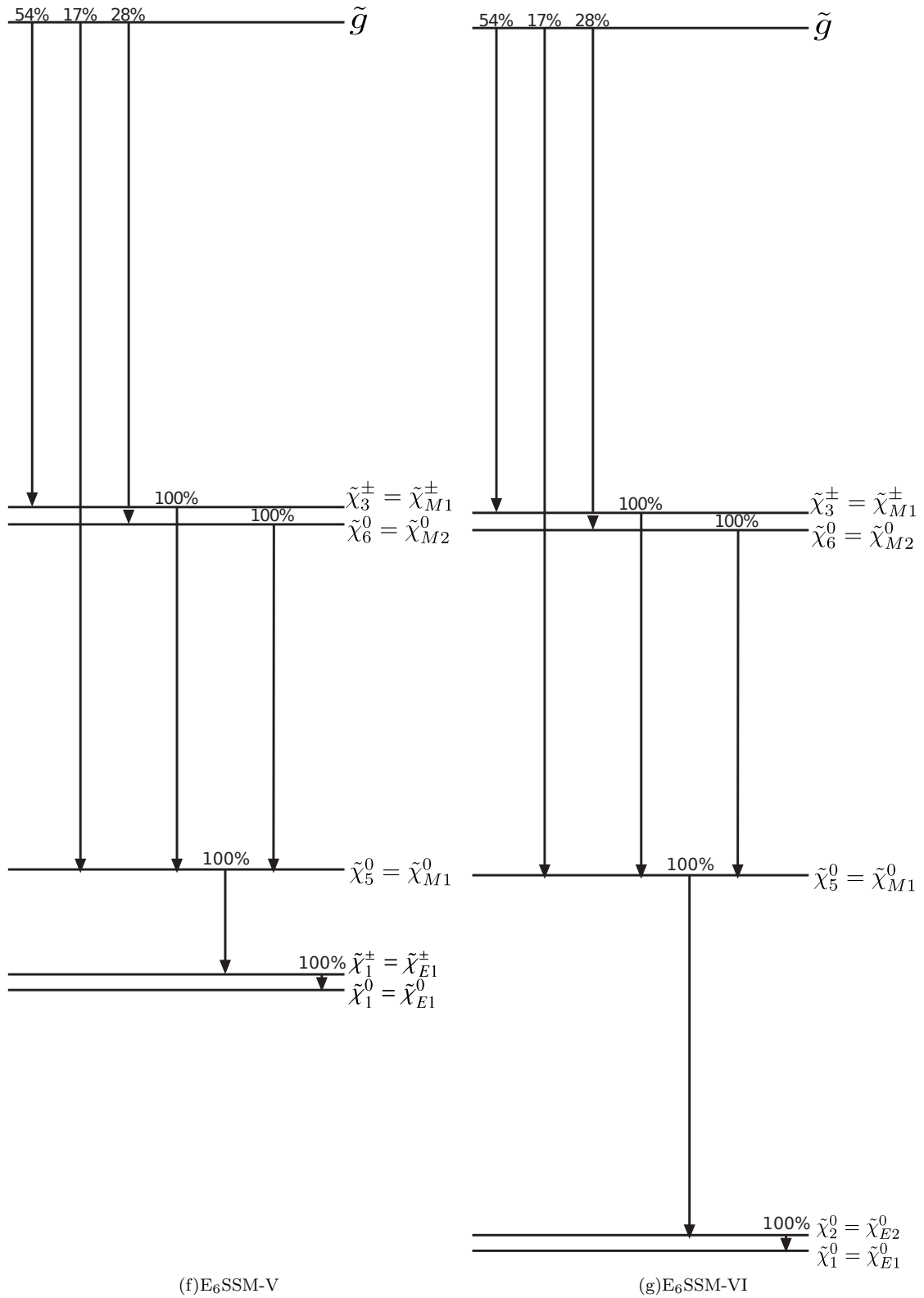


FIG. 15. Gluino decay diagrams for the MSSM and E_6SSM benchmarks, showing the leading decays (contributing more than 90%) for the involved sparticles. The vertical line spacings are proportional to the mass splitting among the particles.

Appendix B: Details about the CalcHEP Model E6SSM-12.02

In this section the contents and properties of the CalcHEP model E6SSM-12.02 (hepmdb:1112.0106)[47] are described in detail. The model files are accessible from HEPMDB [30] where one can either run it with CalcHEP on the IRIDIS cluster via the web interface or download it and run it on one's local CalcHEP installation. The model constitutes of four files; `varsNN.mdl`, `prtclsNN.mdl`, `funcNN.mdl`, and `lgrngNN.mdl`; for input variables, particle definitions, functions or constraints, and Feynman rules for vertices, respectively.

1. Particle content

The model shares many features and particles with the MSSM and its extensions, e.g. the USSM or NMSSM, but has a greater particle content. This CalcHEP version of the E₆SSM, E6SSM-12.02, includes particles from the three generations of 27 representations but not all. What is yet to be implemented is the full Higgs sector, including the *inert* Higgs *boson* states, and the coloured exotics. This is work in progress and will be added in a later version of the model. The extra particles included compared to the MSSM are a SM-singlet S , which mixes with the two MSSM-like CP-even Higgs particles; a Z' -boson; two extra chargino states from inert Higgsinos; and 8 extra neutralino states, two from the bino' and the singlino and six from the inert neutral Higgsinos and singlinos. The CalcHEP particle names and properties as used in the `prtclsNN.mdl` file are shown in Tab. VII. The table shows the full name of each particle followed by the symbols used in CalcHEP for it and its antiparticle. The PDG code is a positive number assigned to each particle for referencing in the code, the antiparticles have PDG codes equal to the negative of the particles' PDGs. The spin, mass, width and color properties are also given in CalcHEP notation. Following the convention from earlier SUSY models in CalcHEP, superpartners, i.e. particles which are odd under R -parity, are denoted with a \sim prefix. The conventions we use for the particle mass and width variables are $M\langle$ particle symbol \rangle and $w\langle$ particle symbol \rangle . If the particle is charged the particle symbol is modified with a suffix $-c$ for "charged" to avoid confusion, e.g. MHc for the charged Higgs H^\pm . In the case of superpartners the \sim is not used in the mass or width variable. Instead a prefix $S-$ or suffix $-o$ is attached to the particle name depending on whether the sparticle is a **S**fermion or a **S**boson, e.g. MGo for the gluino mass and $MSe1$ for the first selectron mass. A number is added to the variable name whenever it refers to particles for which there are more than one of the same type, e.g. neutralinos or stops. We try to keep as close as possible to these conventions without departing too much from conventions used in earlier SUSY models. There are still some deviations from the set up conventions, e.g. the charged slepton sector, which we hope will not be too confusing until a more uniform way of naming the particles and variables is introduced. In future versions of the model the conventions will be used more strictly.

2. Input parameters

The input parameters used in the model, with the exception of some SM parameters, are listed in Tab. VIII. The pseudoscalar Higgs mass is used as an input variable instead of the soft trilinear lambda coupling from the term $A_\lambda \lambda S H_d H_u$. The electroweak soft gaugino masses M_1 , M_2 , and M'_1 are denoted $MG1$, $MG2$, and $MG1b$, respectively. The physical gluino mass is denoted MGo . The soft squark masses for the first two generations are set by a common squark mass scale, MSq , by default. It is however easy to modify the model files by moving the soft squark masses $Mq1$, $Mq2$, $Mu1$, $Mu2$, $Md1$, $Md2$ from the function file `funcNN.mdl` to the input parameter file `varsNN.mdl` and assigning them separate values.

3. Functions and dependent parameters

In the file `funcNN.mdl` all dependent parameters are listed in terms of input parameters and dependent parameters above themselves in the list. The dependence can be given as simple algebraic expressions or as functions of external functions. As an example, expressions for mass matrix elements are given in this file. These matrix elements are then used as inputs for numerical diagonalisation routines from the SLHApplus library, which comes with CalcHEP. SLHApplus then returns evaluated particle masses, which are defined in this file. As an example of what the contents of this file look like, a few lines from it are presented in Tab. IX.

Full Name	particle	antiparticle	PDG ID	2×spin	mass	width	color
gluon	G	G	21	2	0	0	8
neutrino	n1	N1	12	1	0	0	1
electron	e1	E1	11	1	Me1	0	1
muon-neutrino	n2	N2	14	1	0	0	1
muon	e2	E2	13	1	Me2	0	1
tau-neutrino	n3	N3	16	1	0	0	1
tau-lepton	e3	E3	15	1	Me3	0	1
u-quark	u	U	2	1	Mu	0	3
d-quark	d	D	1	1	Md	0	3
c-quark	c	C	4	1	Mc	0	3
s-quark	s	S	3	1	Ms	0	3
t-quark	t	T	6	1	Mt	!wt	3
b-quark	b	B	5	1	Mb	0	3
light Higgs	h1	h1	25	0	Mh1	!wh1	1
heavier Higgs	h2	h2	26	0	Mh2	!wh2	1
heaviest Higgs	h3	h3	27	0	Mh3	!wh3	1
pseudoscalar Higgs	ha	ha	28	0	Mha	!wha	1
charged Higgs	H+	H-	37	0	MHc	!wHc	1
photon	A	A	22	2	0	0	1
Z-boson	Z	Z	23	2	MZ	!wZ	1
W-boson	W+	W-	24	2	MW	!wW	1
Z-primed-boson	Zb	Zb	32	2	MZb	!wZb	1
chargino 1	-1+	-1-	1000024	1	MCo1	!wCo1	1
chargino 2	-2+	-2-	1000037	1	MCo2	!wCo2	1
chargino 3	-3+	-3-	1000038	1	MCo3	!wCo3	1
chargino 4	-4+	-4-	1000039	1	MCo4	!wCo4	1
neutralino 1	-o1	-o1	1000022	1	MNo1	0	1
neutralino 2	-o2	-o2	1000023	1	MNo2	!wNo2	1
neutralino 3	-o3	-o3	1000025	1	MNo3	!wNo3	1
neutralino 4	-o4	-o4	1000026	1	MNo4	!wNo4	1
neutralino 5	-o5	-o5	1000027	1	MNo5	!wNo5	1
neutralino 6	-o6	-o6	1000028	1	MNo6	!wNo6	1
neutralino 7	-o7	-o7	1000029	1	MNo7	!wNo7	1
neutralino 8	-o8	-o8	1000030	1	MNo8	!wNo8	1
neutralino 9	-o9	-o9	1000031	1	MNo9	!wNo9	1
neutralino 10	-oA	-oA	1000032	1	MNoA	!wNoA	1
neutralino 11	-oB	-oB	1000033	1	MNoB	!wNoB	1
neutralino 12	-oC	-oC	1000034	1	MNoC	!wNoC	1
gluino	-g	-g	1000021	1	MGo	!wGo	8
1st selectron	-e1	-E1	1000011	0	MSe1	!wSe1	1
2nd selectron	-e4	-E4	2000011	0	MSe2	!wSe2	1
1st smuon	-e2	-E2	1000013	0	MSmu1	!wSmu1	1
2nd smuon	-e5	-E5	2000013	0	MSmu2	!wSmu2	1
1st stau	-e3	-E3	1000015	0	MStau1	!wStau1	1
2nd stau	-e6	-E6	2000015	0	MStau2	!wStau2	1
e-sneutrino	-n1	-N1	1000012	0	MSn1	!wSn1	1
mu-sneutrino	-n2	-N2	1000014	0	MSn2	!wSn2	1
tau-sneutrino	-n3	-N3	1000016	0	MSn3	!wSn3	1
1st u-squark	-u1	-U1	1000002	0	MSu1	!wSu1	3
2nd u-squark	-u2	-U2	2000002	0	MSu2	!wSu2	3
1st d-squark	-d1	-D1	1000001	0	MSd1	!wSd1	3
2nd d-squark	-d2	-D2	2000001	0	MSd2	!wSd2	3
1st c-squark	-c1	-C1	1000004	0	MSc1	!wSc1	3
2nd c-squark	-c2	-C2	2000004	0	MSc2	!wSc2	3
1st s-squark	-s1	-S1	1000003	0	MSs1	!wSs1	3
2nd s-squark	-s2	-S2	2000003	0	MSs2	!wSs2	3
1st t-squark	-t1	-T1	1000006	0	MSt1	!wSt1	3
2nd t-squark	-t2	-T2	2000006	0	MSt2	!wSt2	3
1st b-squark	-b1	-B1	1000005	0	MSb1	!wSb1	3
2nd b-squark	-b2	-B2	2000005	0	MSb2	!wSb2	3

TABLE VII. Particle content in the E6SSM-12.02 with CalcHEP naming conventions and properties.

Name	Value	Comment
g1b	0.073	U(1)-primed coupling with sqrt(1/40)
hL	0.393	Yukawa coupling for S Hu Hd
hL22	-0.000357	Yukawa coupling for S Hd2 Hu2
hL21	0.04	Yukawa coupling for S Hd2 Hu1
hL12	0.0321	Yukawa coupling for S Hd1 Hu2
hL11	0.000714	Yukawa coupling for S Hd1 Hu1
hFd22	0.001	Yukawa coupling for S2 Hd Hu2
hFd21	0.6844	Yukawa coupling for S2 Hd Hu1
hFd12	0.65	Yukawa coupling for S1 Hd Hu2
hFd11	0.001	Yukawa coupling for S1 Hd Hu1
hFu22	0.001	Yukawa coupling for S2 Hu Hd2
hFu21	0.67	Yukawa coupling for S2 Hu Hd1
hFu12	0.64	Yukawa coupling for S1 Hu Hd2
hFu11	0.001	Yukawa coupling for S1 Hu Hd1
hXd2	0.000714	Yukawa coupling for S Hd Hu2
hXd1	0.000714	Yukawa coupling for S Hd Hu1
hXu2	0.000714	Yukawa coupling for S Hd2 Hu
hXu1	0.000714	Yukawa coupling for S Hd1 Hu
hZ2	0.001	Yukawa coupling for S2 Hd Hu
hZ1	0.001	Yukawa coupling for S1 Hd Hu
Svev	5180	SM-singlet VEV
Hvev	246	SM Higgs VEV
MSq	2000	Common soft squark mass scale for gen. 1 and 2 = Mq1= Mq2= Mu1= Mu2= Md1= Md2
topA	-2200	soft trilinear A-coupling for top
botA	-2200	soft trilinear A-coupling for bottom
Mq3	2000	Soft squark mass for third gen. SU(2) doublet, q
Mu3	2000	Soft squark mass for third gen. right-handed u
Md3	2000	Soft squark mass for third gen. right-handed d
Ml1	2000	Soft slepton mass for 1st gen. SU(2) doublet, L
Ml2	2000	Soft slepton mass for 2nd gen. SU(2) doublet, L
Ml3	2000	Soft slepton mass for 3rd gen. SU(2) doublet, L
Mr1	2000	Soft slepton mass for 1st gen. right-handed e (selectron)
Mr2	2000	Soft slepton mass for 2nd gen. right-handed e (smuon)
Mr3	2040	Soft slepton mass for 3rd gen. right-handed e (stau)
tauA	-2200	soft trilinear A-coupling for tau
lsc	165	scale for Higgs loop corrections
lmt	165	top mass in Higgs loop corrections
Mha	2736	pseudoscalar Higgs mass
MG1	150	Soft gaugino mass for U(1) (hypercharge)
MG2	300	Soft gaugino mass for SU(2)
MG1b	151	Soft gaugino mass for U(1)'
Maux	1	mass of aux particles
tb	1.5	tangent beta
MGo	800	gluino mass

TABLE VIII. Input parameters for the E6SSM-12.02 model in CalcHEP notation. Some SM parameters have been removed from this list. This is the format and content of the varsNN.mdl file that comes with the model. By default the parameter values of benchmark E6SSM-I are given.

Name	Expression
⋮	⋮
MNE13	-MZ*SW*cb
MNE14	MZ*SW*sb
⋮	⋮
MNo1	MassArray(NeDiag, 1) % Neutralino mass 1
MNo2	MassArray(NeDiag, 2) % Neutralino mass 2
⋮	⋮

TABLE IX. Example lines from the model file funcNN.mdl, where dependent parameters are specified. Comments are allowed at the ends of lines after a %. The lines shown are examples of simple expressions for matrix elements and masses defined by external numerical routines.

P1	P2	P3	P4	Factor	dLagrangian/ dA(p1) dA(p2) dA(p3)
A	H+	H-		-EE	m1.p2-m1.p3
G	W+	-C1	-b1	-EE*GG*sqrt2*Vcb*Zd33/SW	m1.m2
W+	W+	W-	W-	-EE^2/SW^2	m1.m4*m2.m3-2*m1.m2*m3.m4+m1.m3*m2.m4

TABLE X. Example lines from the model file `lgrngNN.mdl`, where Feynman rules for all vertices in the model are listed.

4. Feynman rules

All of the vertices in the model are listed in the file `lgrngNN.mdl`. Some of the vertices include auxiliary particles, which are included for technical reasons, e.g. to construct a four-gluon vertex. Examples of vertices and Feynman rules from this file are given in Tab. X.

-
- [1] D. Chung, L. Everett, G. Kane, S. King, J. D. Lykken, *et al.*, Phys.Rept. **407**, 1 (2005), arXiv:hep-ph/0312378 [hep-ph].
- [2] G. Aad *et al.* (ATLAS Collaboration), (2011), arXiv:1109.6572 [hep-ex].
- [3] S. Chatrchyan *et al.* (CMS Collaboration), (2011), arXiv:1109.2352 [hep-ex].
- [4] S. Chatrchyan *et al.* (CMS Collaboration), (2011), * Temporary entry *, arXiv:1107.1870 [hep-ex].
- [5] H. Okawa and for the ATLAS Collaboration, (2011), 1110.0282.
- [6] U. Ellwanger, C. Hugonie, and A. M. Teixeira, Phys.Rept. **496**, 1 (2010), arXiv:0910.1785 [hep-ph].
- [7] S. King, S. Moretti, and R. Nevzorov, Phys.Rev. **D73**, 035009 (2006), arXiv:hep-ph/0510419 [hep-ph].
- [8] S. King, S. Moretti, and R. Nevzorov, Phys.Lett. **B634**, 278 (2006), arXiv:hep-ph/0511256 [hep-ph].
- [9] *Update on the Standard Model Higgs searches in ATLAS*, Tech. Rep. ATLAS-CONF-2012-093 (CERN, Geneva, 2012).
- [10] *Update on the Standard Model Higgs searches in CMS*, Tech. Rep. CMS-PAS-HIG-12-020 (CERN, Geneva, 2012).
- [11] P. Athron, S. King, . Miller, D.J., S. Moretti, R. Nevzorov, *et al.*, Phys.Lett. **B681**, 448 (2009), arXiv:0901.1192 [hep-ph].
- [12] P. Athron, S. King, D. Miller, S. Moretti, and R. Nevzorov, Phys.Rev. **D80**, 035009 (2009), arXiv:0904.2169 [hep-ph].
- [13] P. Athron, S. King, D. Miller, S. Moretti, and R. Nevzorov, Phys.Rev. **D84**, 055006 (2011), arXiv:1102.4363 [hep-ph].
- [14] S. King, S. Moretti, and R. Nevzorov, Phys.Lett. **B650**, 57 (2007), arXiv:hep-ph/0701064 [hep-ph].
- [15] S. King, R. Luo, . Miller, D.J., and R. Nevzorov, JHEP **0812**, 042 (2008), arXiv:0806.0330 [hep-ph].
- [16] J. Kalinowski, S. King, and J. Roberts, JHEP **0901**, 066 (2009), arXiv:0811.2204 [hep-ph].
- [17] J. P. Hall and S. F. King, JHEP **0908**, 088 (2009), arXiv:0905.2696 [hep-ph].
- [18] E. Accomando, A. Belyaev, L. Fedeli, S. F. King, and C. Shepherd-Themistocleous, Phys.Rev. **D83**, 075012 (2011), arXiv:1010.6058 [hep-ph].
- [19] S. Chatrchyan *et al.* (CMS Collaboration), (2012), arXiv:1206.1849 [hep-ex].
- [20] P. Athron, S. King, D. Miller, S. Moretti, and R. Nevzorov, (2012), arXiv:1206.5028 [hep-ph].
- [21] S. Chatrchyan *et al.* (CMS Collaboration), Phys.Lett. **B704**, 123 (2011), arXiv:1107.4771 [hep-ex].
- [22] J. Hall, S. King, R. Nevzorov, S. Pakvasa, M. Sher, *et al.*, Phys.Rev. **D83**, 075013 (2011), arXiv:1012.5114 [hep-ph].
- [23] E. Aprile *et al.* (XENON100 Collaboration), Phys.Rev.Lett. **107**, 131302 (2011), arXiv:1104.2549 [astro-ph.CO].
- [24] J. P. Hall and S. F. King, JHEP **1106**, 006 (2011), arXiv:1104.2259 [hep-ph].
- [25] S. F. King and A. Merle, (2012), arXiv:1205.0551 [hep-ph].
- [26] E. Komatsu *et al.* (WMAP Collaboration), Astrophys.J.Suppl. **192**, 18 (2011), arXiv:1001.4538 [astro-ph.CO].
- [27] E. Aprile *et al.* (XENON100 Collaboration), (2012), arXiv:1207.5988 [astro-ph.CO].
- [28] A. Semenov, (2010), 1005.1909.
- [29] G. Belanger, N. D. Christensen, A. Pukhov, and A. Semenov, Comput.Phys.Commun. **182:763-774,2011** (2010), 1008.0181.
- [30] A. Belyaev *et al.*, “Hepmdb,” <https://hepmdb.soton.ac.uk>.
- [31] J. Pumplin *et al.*, JHEP **07**, 012 (2002), arXiv:hep-ph/0201195.
- [32] W. Beenakker, R. Hopker, M. Spira, and P. Zerwas, Nucl.Phys. **B492**, 51 (1997), arXiv:hep-ph/9610490 [hep-ph].
- [33] A. Kulesza and L. Motyka, Phys.Rev. **D80**, 095004 (2009), arXiv:0905.4749 [hep-ph].
- [34] W. Beenakker, S. Brensing, M. Kramer, A. Kulesza, E. Laenen, *et al.*, JHEP **0912**, 041 (2009), arXiv:0909.4418 [hep-ph].
- [35] W. Beenakker, S. Brensing, M. Kramer, A. Kulesza, E. Laenen, *et al.*, Int.J.Mod.Phys. **A26**, 2637 (2011), arXiv:1105.1110 [hep-ph].
- [36] N. C. Alexander Pukhov, Alexander Belyaev, “CalcHEP 2.5 – the ready setup for collider physics,” In preparation.
- [37] S. Chatrchyan *et al.* (CMS Collaboration), (2011), CMS-PAS-SUS-11-004.
- [38] G. Aad *et al.* (ATLAS Collaboration), Phys.Rev. **D85**, 012006 (2012), 18 pages plus author list (30 pages total), 9 figures, 4 tables, final version to appear in Physical Review D, arXiv:1109.6606 [hep-ex].
- [39] G. Aad *et al.* (ATLAS Collaboration), (2011), arXiv:1110.6189 [hep-ex].
- [40] S. Chatrchyan *et al.* (CMS Collaboration), (2011), CMS-PAS-SUS-11-013.
- [41] *Search for supersymmetry in events with four or more leptons and missing transverse momentum in pp collisions at $\sqrt{s} = 7$ TeV with the ATLAS detector*, Tech. Rep. ATLAS-CONF-2012-001 (CERN, Geneva, 2012).

- [42] H. Baer, H. Prosper, and H. Summy, *Phys.Rev.D* **77:055017,2008** (2008), 0801.3799.
- [43] V. Bartsch and G. Quast, *Expected Signal Observability at Future Experiments*, Tech. Rep. CMS-NOTE-2005-004 (CERN, Geneva, 2005).
- [44] S. I. Bityukov and N. V. Krasnikov, (2007), physics/9809037.
- [45] *Search for squarks and gluinos with the ATLAS detector using final states with jets and missing transverse momentum and 5.8 fb⁻¹ of $\sqrt{s}=8$ TeV proton-proton collision data*, Tech. Rep. ATLAS-CONF-2012-109 (CERN, Geneva, 2012).
- [46] J. Conway *et al.*, “Pgs 4,” <http://www.physics.ucdavis.edu/conway/research/software/pgs/pgs4-general.htm>.
- [47] J. P. Hall and P. Svantesson, “E6ssm-12.02,” <http://hepmb.soton.ac.uk/hepmb:1112.0106>, calcHEP model.